

Diplomarbeit

Dynamic Modeling of PEM Fuel Cells

ausgeführt zum Zwecke der Erlangung des akademischen Grades eines Diplom-Ingenieurs
unter der Leitung von

Univ.Prof. Dr. Stefan Jakubek
Institut für Mechanik und Mechatronik
E325 A5

eingereicht an der Technischen Universität Wien

Fakultät für Maschinenwesen und Betriebswissenschaften

von

Florian Lohninger
Matr.Nr.: 0651697
Königswiesen 5
4880 St. Georgen i.Att.

Wien, am 27. Januar 2014

Florian Lohninger

Eidesstattliche Erklärung

Ich erkläre eidesstattlich, dass ich die Arbeit selbständig angefertigt, keine anderen als die angegebenen Hilfsmittel benutzt und alle aus ungedruckten Quellen, gedruckter Literatur oder aus dem Internet im Wortlaut oder im wesentlichen Inhalt übernommenen Formulierungen und Konzepte gemäß den Richtlinien wissenschaftlicher Arbeiten zitiert, durch Fußnoten gekennzeichnet bzw. mit genauer Quellenangabe kenntlich gemacht habe.

Wien, am 27. Januar 2014

Florian Lohninger

Danksagung

Ich möchte mich bei der Firma AVL List GmbH in Graz bedanken, die ihre Kapazitäten zur Erstellung dieser Arbeit bereitgestellt hat. Die Zusammenarbeit hat in allen Belangen immer ausgezeichnet funktioniert und entscheidend zur Entstehung dieser Arbeit beigetragen. Im Speziellen bedanke ich mich bei Dr. Reinhard Tatschl für die Zieldefinition meiner Arbeit, für die inhaltliche und organisatorische Betreuung bei Dipl.-Ing.(FH) Christoph Kügele, für die wesentliche Unterstützung meiner Arbeit bei Dr. Johann Wurzenberger sowie Dipl. Phys. Sophie Bardubitzki und bei Dr. Clemens Fink für die wissenschaftliche Beratung.

Weiters richte ich meinen Dank an die Technische Universität Wien, im Speziellen hierbei an meinen Diplomarbeitsbetreuer Univ.Prof. Dipl.-Ing. Dr.techn. Stefan Jakubek, der die Verbindung zur AVL List GmbH erst ermöglicht hat und bei allen inhaltlichen wie wissenschaftlichen Belangen stets ein Ansprechpartner war.

Kurzfassung

Der Zweck dieser Diplomarbeit war die Modellerstellung eines Niedertemperatur Protonentauschmembran -Brennstoffzellen (PEMFC) Stacks. Das Ergebnis ist ein Modell, das diskrete eindimensionale Gaskanäle an Anode und Kathode transient simuliert. In Verbindung mit einem zusätzlichen Rechenkern, erstellt in C-Code, werden alle restlichen Parameter berechnet. Die Modellstruktur wurde in BoostRT implementiert, einem von der AVL List GmbH bereitgestellten Programm, und als weitere Option steht ein Betrieb in Matlab/Simulink zur Verfügung.

Die Kapitel 1,2 und 3 erläutern wie PEMFC funktionieren und wie sie mathematisch beschrieben werden. Prinzipiell findet in einer PEMFC eine Reaktion statt die chemische Energie in elektrische Energie und Hitze umwandelt. Dieser Prozess wird im wesentlichen mit einem System von partiellen Differenzialgleichungen beschrieben und je nach Zellschicht mit Quellen und Senken modifiziert. 3D Modelle sind aufgrund der zahlreichen physikalischen Effekte jedoch nicht im zeitnahen Bereich.

Somit wurde eine Reduktion durchgeführt welche in Kapitel 4 und 5 dokumentiert ist. Es entstand ein Modell in BoostRT, bei dem auf vorhandene Simulationsbausteine, genannt Catalyst Core und Catalyst Substrate, zurückgegriffen wurde. In Kombination können diese thermodynamische, chemische und strömungsmechanische Effekte in einer Gasströmung und deren Umgebung abbilden, die durch katalytische Reaktionen beeinflusst werden. Diese Elemente wurden ergänzt um einen PEMFC spezifischen Rechenkern.

In Kapitel 6 folgt die Modellkalibrierung und Validierung. Die Referenzzelle mit den dazugehörigen Messdaten wurde aus der Arbeit von Fink [1] übernommen. Im ersten Teil werden die Modellkoeffizienten kalibriert. Der zweite Teil beinhaltet die Analyse der Simulationsergebnisse. Obwohl die durchschnittliche Stromdichte in der Zelle korrekt wiedergegeben wurde, stimmte die Verteilung entlang der diskreten Elemente des Kanals nicht. Als entscheidender Effekt wurde der variable Massenstrom in den Gaskanälen identifiziert, der durch die Core Elemente als konstant angenommen wird.

Trotzdem zeigt die Struktur des Modells die Fähigkeiten einer 1D Modellierung und liefert eine Basis für weitere Verbesserungen. Diese betreffen die Annahme des konstanten Massenstroms im Core und da die Membran die Elektrodynamik der PEMFC beeinflusst, den Membran spezifischen Teil im Berechnungskern.

Abstract

The purpose of this diploma thesis is to create a model of a low temperature Proton Exchange Membrane Fuel Cell (PEMFC) Stack. The result is a model which simulates discrete one-dimensional anode and cathode gas channels in combination with a calculation kernel, coded in C-Code, that computes fuel cell specific parameters. The operating environment is BoostRT, a program provided by the AVL List GmbH and, as additive option, it can be run from Matlab/Simulink.

Chapters 1,2 and 3 start with a holistic approach of how PEM Fuel Cells work and how they are mathematically modeled. The basic procedure of a fuel cell is the transformation of chemical energy into electrical energy and heat. This process is described with a set of partial differential equations, called "conservation equations" adopted with sink and source terms depending on the current cell layer modeled. But due to the numerous physical effects occurring in a PEMFC, a 3D model was not capable of short simulation times.

Consequently, in chapters 4 and 5 a model reduction is carried out. Therefore the strategy was to use existing simulation components of the program BoostRT. The elements are called Core and Substrate. Linked together, they can simulate transient gas streams affected by catalytic reactions combined with thermodynamic effects on the surrounding solid material. Supplemented with the C-Code calculation kernel the components are interconnected for the calculation of the remaining parameters.

The model calibration and validation is documented in chapter 6. The reference cell and measurements were chosen from the work of Fink [1]. In the first part the model coefficients are modified. In the second part the simulation results are analyzed and even though the average outcome of the cell current density is correct, the current density distribution along the channel shows divergences. The divergences are due to the fact that the mass stream in a PEMFC gas stream channel is variable, while the core element assumes a constant mass stream.

Even though the structure of the model shows the capabilities of a 1D model and provides a basis for additional developments. In constitutive projects the gas stream should be adapted and as the membrane influences the electrodynamics of a PEM Fuel Cell, the membrane specific calculation code could be improved further.

Contents

1	Introduction	1
1.1	Topic of the Diploma Thesis	1
1.2	Introduction to Fuel Cells	1
1.3	Why a PEM Fuel Cell Stack Model	3
2	Architecture and Physical Effects of PEM Fuel Cells	4
2.1	Architecture of a PEM Fuel Cell	4
2.1.1	Bipolar Plates, BP	6
2.1.2	Gas Diffusion Layer, GDL	7
2.1.3	Catalytic Layer, CL	7
2.1.4	Polymer Electrolyte Membrane, PEM	8
2.1.5	Stack Design	9
2.2	Physical Effects of a PEM Fuel Cell	10
2.2.1	Thermodynamics	10
2.2.2	Electrochemics	11
2.2.3	Charge Transport	14
2.2.4	Gas Dynamics	14
2.2.5	Water Management	14
2.2.6	Heat Losses	15
3	Modeling a PEM Fuel Cell	16
3.1	Continuity equation	16
3.2	Momentum Conservation	17
3.3	Conservation of Energy	19
3.4	Conservation of Species	20
3.5	Conservation of Charge	21
3.6	Ideal Gas Law	23
4	Development of the Model Concept	24
4.1	Model Requirements	24
4.2	Model Concept	24
4.2.1	The Simulation Environment BOOST RT	26
4.2.2	The PEM Calculation Core encoded in C-Code	26
4.3	The Model Capabilities	26

5	The PEM Fuel Cell Model in BOOST RT	28
5.1	The Electrochemical Model in BOOST RT	28
5.1.1	Theoretical Voltage	28
5.1.2	The Implementation of the Butler-Volmer Equation	29
5.1.3	Ohmic and Ionic Losses	30
5.1.4	Concentration Losses	35
5.1.5	Cell Potential	35
5.2	The Thermal Model in BOOST RT	36
5.2.1	Cell Potential with Hydrogen's HHV	37
5.2.2	Fuel Cell Heat Generation	37
5.2.3	Cooling Power of the Active Cooling System	38
5.2.4	Calculation of Temperature Changes	39
5.2.5	The Catalyst Substrate	40
5.3	Modeling of the Gas Channels	40
5.3.1	Species Turnover	40
5.3.2	The Catalyst Core	41
5.4	The C-Code Calculation Kernel or PEM Core	41
6	Model Configuration and Validation	44
6.1	General Configuration of BOOST RT, -Program and -Model	44
6.1.1	General Preparation of BOOST RT	44
6.1.2	General Model Configuration	45
6.2	Model Configuration and Fitting	55
6.2.1	The PEM Fuel Cell and the Reference Case	57
6.2.2	BOOST RT GUI Parameters for the Reference Case	60
6.3	Model Validation	63
6.3.1	Simulation of the Reference Case	63
6.3.2	Pressure Variation	68
6.3.3	Different Humidification	70
6.3.4	Different Stoichiometry	71
6.4	Result Interpretation and Compendium	73
7	Possible further Model Development	74
7.1	Catalyst Core Adaptations	74
7.2	Advanced Membrane Model	74
	Bibliography	76

List of Figures

1.1	Fuel cell stack from Ballard Power Systems [2]	2
1.2	Complete fuel cell systems from Ballard Power Systems [2]	3
2.1	Structure of a PEM fuel cell (Not true to scale) [1]	5
2.2	Cross section of a PEM fuel cell [3]	6
2.3	Exemplary gas channel architectures [4]	7
2.4	Catalytic layer three phase region [5]	8
2.5	Chemical structural formula of Nafion [®] [6]	9
2.6	Stack architecture [7]	10
2.7	Polarization curve [8]	12
2.8	Charge double layer [9]	13
2.9	Phase lags due to the charge double layer [10]	13
4.1	The BOOST RT PEM fuel cell stack model	25
5.1	Additional PEM Catalyst Core data buses	42
5.2	PEM Catalyst Core output data	43
6.1	Configuration of the kernel	45
6.2	Pressure driven model configuration	46
6.3	Mass flow driven model configuration	47
6.4	Anode Inlet Ambient	48
6.5	Catalyst Core element	50
6.6	Catalyst Substrate element	51
6.7	Constants element	51
6.8	The C-Interface input and output ports	52
6.9	Data Bus Connections	53
6.10	CMC element	54
6.11	The IMPRESS Chart	55
6.12	Model configuration	56
6.13	PEM fuel cell used for the validation [1]	58
6.14	Reference case experiment measurements	60
6.15	Reference case anode Catalyst Core configuration	61
6.16	Reference case anode Catalyst Substrate configuration	61
6.17	Reference case cathode Catalyst Core configuration	62
6.18	Reference case cathode Catalyst Substrate configuration	62

6.19	Reference case Constants 1 configuration	63
6.20	Simulation of the reference case	64
6.21	Current densities along the channel	64
6.22	Mass fractions of H_2	65
6.23	Mass fractions of O_2	65
6.24	Mass fraction of O_2 in the last cathode gas channel element	67
6.25	Mass flow in the cathode gas channel	67
6.26	Cell average current density plotted over time	68
6.27	Simulation at 1.2 bar	69
6.28	Current densities along the channel	69
6.29	Simulation at 0.6/0.6	70
6.30	Current Densities along the channel	71
6.31	Simulation with lambda 4	72
6.32	Current densities along the channel	72

Chapter 1

Introduction

1.1 Topic of the Diploma Thesis

The topic of the Diploma Thesis was to create a model of a PEM fuel cell stack (PEM for Polymer Electrolyte Membrane or Proton Exchange Membrane) which can be operated from Matlab/Simulink [11]. It was created in cooperation between the AVL List GmbH [12] and the TU Vienna Institute for Control Theory and Process Automation [13].

1.2 Introduction to Fuel Cells

Fuel cells are electro-galvanic elements capable of producing electric power directly out of chemical energy. As side product heat is released due to the reaction entropies of several components. If the heat can be used, fuel cells reach high efficiency factors. Compared to batteries fuel cells are supported with the chemical reaction elements and as long the support is sustained energy can be generated. Due to the direct conversion from chemical to electric energy, they are not limited by the Carnot Factor, especially when it comes to low temperature fuel cells.[14] While this work concentrates only on low temperature PEM fuel cells there exist several other types of fuel cells.[15]

PEM fuel cells, modeled in this thesis, belong to the group of low temperature fuel cells which are typically operated in a temperature range between 60°C to 80°C. The reaction components are hydrogen H_2 and oxygen O_2 and the only byproduct at the end of the process is water H_2O . PEMFCs are a promising candidate to replace several types of batteries and in general can lead to the reduction of the use of fossil fuels. Hydrogen is the most abundant element in the universe and it appears in nature in its molecular form H_2 . However, the predominant amount is bound in water and almost all organic compounds, whereas a PEM fuel cell needs pure H_2 . Here on earth it has to be produced since it does not appear in sufficient quantities. There are several methods of producing H_2 and often it results as side product in chemical production procedures. If the energy for the H_2 production is generated

in a renewable, ecological way, fuel cells can support the transition to a renewable energy supplied society. A closer look at the need of fuel cells and an analysis of the several types of fuel cells was done by Song [16].

In a PEMFC the chemical reactant gases are supplied and are separated by the PEM. At the anode catalyst layer, the H_2 molecules are separated into protons and electrons. The electrons flow through the electric conducting circuit, the protons can move through the PEM. At the cathode catalyst layer, O_2 molecules are separated into their atomic components and with the protons and electrons they react to clean water. During the process heat is generated and the whole process only sustains if the membrane stays hydrated.

The amount of energy released by a PEMFC depends on the cell area. A cell can be operated up to a power density of around $0.6 \text{ W}\cdot\text{cm}^{-2}$. The voltage range, typically, is in between 0.8 to 0.5 V and the current density is in between 0.5 to $1 \text{ A}\cdot\text{cm}^{-2}$. Depending on the power needed the cell reaction areas are increased or/and are serially combined in order to realize higher voltages. This so combined cell packs are called Fuel Cell Stacks. Due to the comfortable sizing possibilities of fuel cells they can be built for a wide range of power requirements starting at some W e.g. for the use in mobile phones, and going up to hundreds of kW for the stationary use. Depending on the size of the system a passive cooling can be sufficient but especially when it comes to bigger fuel cell stacks, an active cooling is necessary.

The basics of PEM fuel cells are investigated in chapter 2.

A fuel cell stack is shown in figure 1.1 which is offered by a main producer of fuel cells, Ballard Power Systems [2]. The stack is sizeable and air-cooled. It has self humidifying membrane electrodes assemblies and is suitable for a wide range of applications. Per cell a power of 45 W can be generated and the average voltage is $683 \text{ mV}\cdot\text{cell}^{-1}$. The time duration to reach 80% of the rated power is 20 seconds.



Figure 1.1: Fuel cell stack from Ballard Power Systems [2]

A complete fuel cell system for significant higher power capabilities is shown in figure

1.2. This stationary power generator provides an energy flow up to 1 MW with zero emissions.



Figure 1.2: Complete fuel cell systems from Ballard Power Systems [2]

1.3 Why a PEM Fuel Cell Stack Model

The operation of a fuel cell stack is a sophisticated task. Several system states have to stay in a vital range to be able to sustain the power supply. A cell model has several tasks but one, though, has to understand, that a physical model is always a simplified reproduction of the real world since no model can include all the appearing physical effects. However, the more effects are modeled the slower the calculations are and so the modeling detail always depends on the operational field.

In this thesis the main intentions were to be able to calculate several operating points of the cell and to be able to control the BoP (BoP for Balance of Plant) components which are usually modeled in the Matlab/Simulink environment. The term BoP comprises all the necessary utilities for the cell which ensures the control of the amount of reaction gases supplied to the cell or they humidify the gases if the PEM is too dry.

Another intended use is, to be able to set up a state observer. A state observer, in the field of control theory, provides an estimated state vector out of some measurements of the systems state. To know the complete state vector is essential for further control applications in, for instance, state vector feedback control theory.

An overview to the common ways of modeling a PEM fuel cell Stack has been given by Haraldsson.[17]

Chapter 2

Architecture and Physical Effects of PEM Fuel Cells

This chapter comprises the basics about a PEM fuel cell. It begins with the architecture of a cell and what the main responsibilities are. Further on the construction of a stack is overviewed and how the cells are combined. Then an overview is provided of the dominant physical effects. The main intention of this chapter is to get a basic understanding of how a PEMFC looks like and what is happening in a cell when a certain operational point is reviewed. Furthermore, it provides information about the main physical effects that are important for the later modeling of the cell. Unfortunately it has not been possible to comprise all physical effects, regarding the range of this work. Especially when it comes to altering effects one would have to search for additional literature.[18]

2.1 Architecture of a PEM Fuel Cell

As PEM fuel cells are still in a stage of intense development, the details of the architecture are continuously improved. The same is true for the materials of which a PEM fuel cell and each of the cell layers are made. To give a first impression, figure 2.1 shows a general construction design of a PEM fuel cell. Here the cell architecture can be subdivided into seven layers or cell domains. Each of the cell layers or domains can be distinguished by the functionalities they have to provide. The layers are made of several different materials which can be further distinguished in shape and porosity.

The outermost or boundary layers are the Bipolar Plates or BP, where the gas channels are located. Then there are the Gas Diffusion Layers, also the GDL, which are made of porous material to distribute gas and to protect the membrane from dehydration. The actual chemical reactions take place in the Catalyst Layers of CL. The presence of the catalyst material lowers the activation energy and helps to sustain a reactive electrode. In the central part of the cell the PEM itself is located. It separates the anode from the cathode and is conductive only for protons if it is sufficiently hydrated. The electrons have to take the way through the electrical circuit

and the released electrical energy can be used.

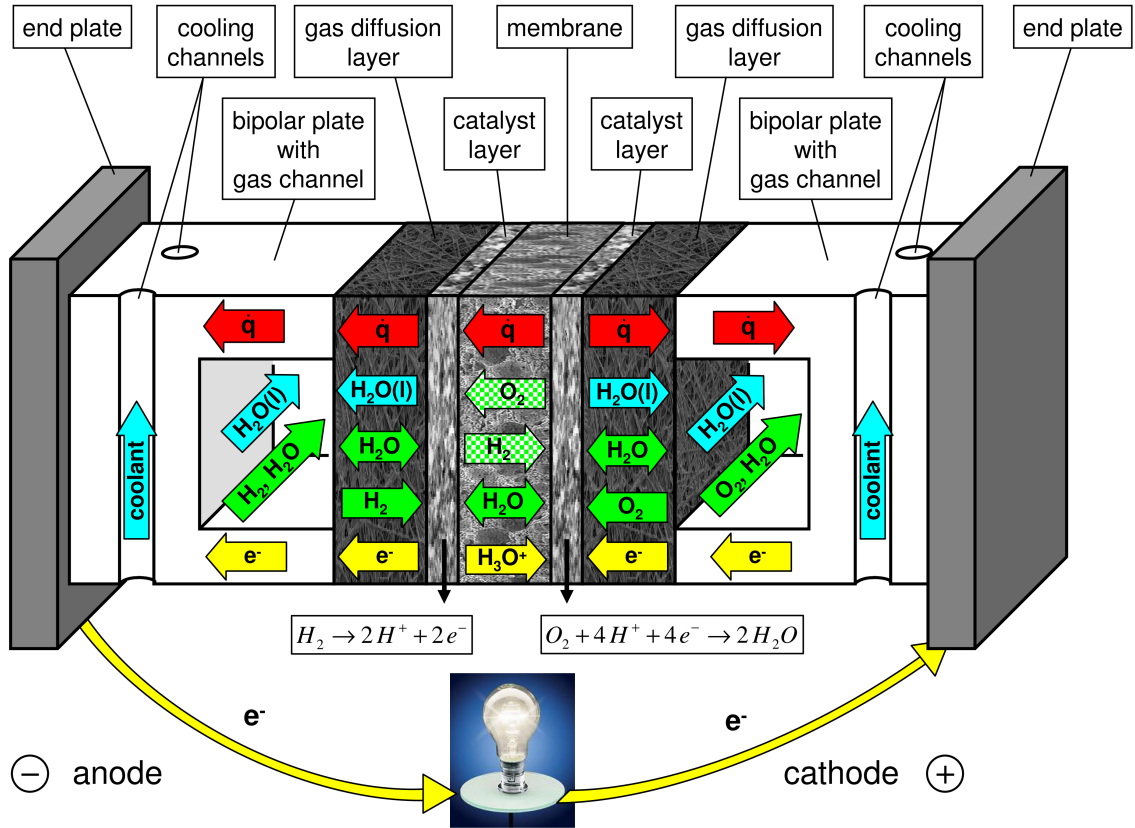


Figure 2.1: Structure of a PEM fuel cell (Not true to scale) [1]

Figure 2.2 gives a closer look at a PEM cell with correct proportions of the several layers and the bright areas mark water drops in the cell. Especially the Bipolar Plates dominate the design if they are compared to the other layers. Between the Catalyst Layers and the GDL there is an additional thin coat called the Micro Porous Layer MPL. The main tasks are to ensure a balanced water management and it should prevent water from creating drops via condensation. These small water drops hinder the free flow of the reaction gases. The MPL consists of PTFE (Polytetrafluoroethylene, also called Teflon).[19] One of the main characteristics of PTFE is its low surface tension which leads to a low water flow resistance. The MEA (Membrane Electrode Assembly) is the overall denomination of the Membrane and Catalyst Layers of anode and cathode.

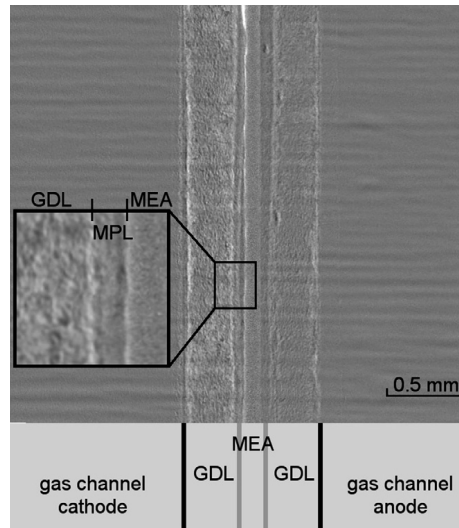


Figure 2.2: Cross section of a PEM fuel cell [3]

The next sections take a deeper look into each of the layers.

2.1.1 Bipolar Plates, BP

The Bipolar Plates are responsible for the transportation of the reaction gases, the conduction of reaction heat and charge conduction. Therefore, they should be big enough to comprise the gas conducting channels and, depending on the cell design, the cooling channels. Of course, the cooling substance has to be non-conductive or separate cooling plates are used which would be placed next to the BPs. Regarding the allocation of the gas channels, literature shows that there are numerous different approaches. The figure 2.3 gives an idea of some possible designs. The search for the optimal balance between the attributes a BP should fulfill has still been the driving force when it comes to the development of new channel geometries. Further information about channel geometry is provided e.g. by Li.[20]

Common materials, which are used for the BP, are graphite or pressed metal plates which can be produced faster. Apart from that, they comprise several of the necessary attributes of BPs like a low resistance for negative charge flow, good heat conduction and high resistance against the diffusion of reaction gases. The uncontrolled leakage of reaction gases is generally more an issue due to insufficient sealing between the layers or of the whole cell.

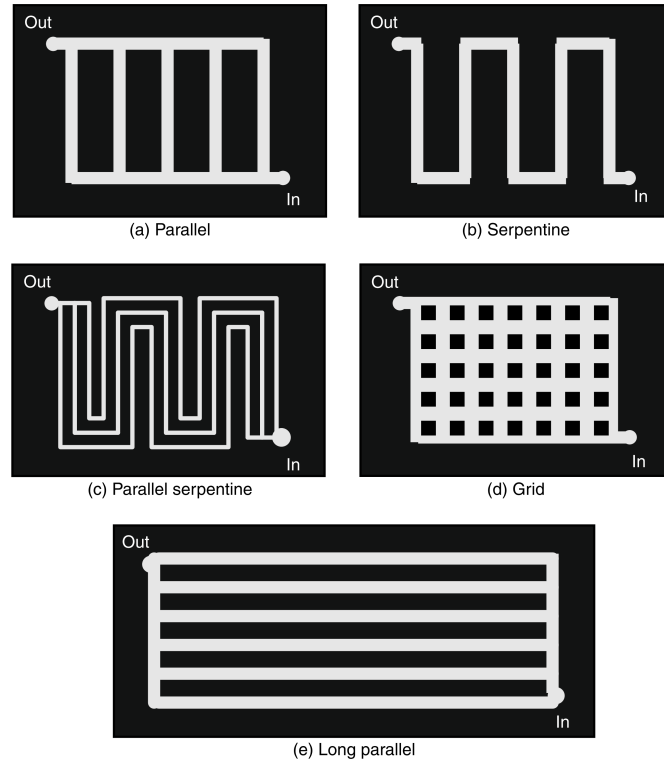


Figure 2.3: Exemplary gas channel architectures [4]

2.1.2 Gas Diffusion Layer, GDL

The purpose of the Gas Diffusion Layer is to distribute the reaction gases over the Catalytic Layer, to conduct electric charges and to ensure an optimal humidity level due to balanced diffusion attributes. In higher developed cells there is a further distinction of the Diffusion Layers in two different porosity grades. This is basically advantageous for diffusion characteristics and the water management which is overall a key factor in PEM fuel cell operation. The membrane should be, under all circumstances, prevented from drying out or from being flooded. In the first case the ionic resistance of the membrane would increase dramatically and in the second case the diffusion of the reaction gases is hindered or even blocked. In both cases the cell power would collapse or even fall to zero. Furthermore the GDL should have a low resistance for the conduction of negative charges as they lie next to the electrodes. All the negative charges created in the electrolytic reactions have to be conducted to the BP.

2.1.3 Catalytic Layer, CL

The catalytic layers mark the electrodes of a PEMFC. Here the reactions occur and, due to the physical principle, they are interconnected with the membrane to form the MEA, Membrane Electrode Assembly. The common material for the catalyst itself is platinum. A close look at the catalyst layers shows, that small platinum particles

are evaporated on a carrier porous material e.g. the GDL. At the beginning of fuel cell development platinum was a main cost factor as huge amounts of platinum were necessary to build a catalyst. Since only the surface counts there has ever been a decrease in the use of platinum which has nowadays come to a level where the cost influence is not significant anymore.

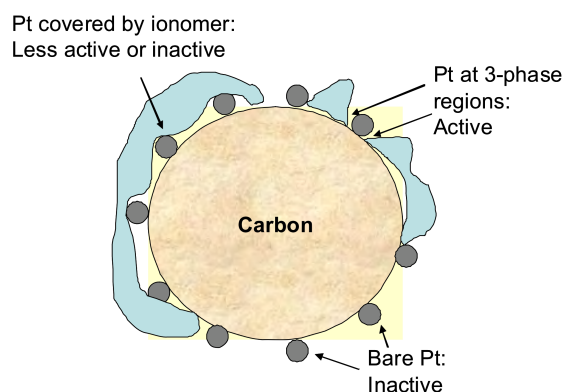


Figure 2.4: Catalytic layer three phase region [5]

Platinum, though, is not enough for starting the reactions. It lowers the activation energy but the reactions occur only at the three phase region, where the PEM, the platinum particles and the gases come together. All three phases have to be present because the electrons can only move through the platinum particle and the carbon, the protons can only move through the PEM and the reaction gases have to be present too. Figure 2.4 shows schematically how the three phase interaction region looks like and how its shape has to be if reactions should occur.

2.1.4 Polymer Electrolyte Membrane, PEM

In the center, the PEM itself is located and as electrolyte it is responsible for separating the anode from the cathode. The dynamics and the performance of a cell are mainly driven by the physical behavior of the PEM.[21] Essential attributes are high chemical constancy, high conductivity for protons and preventing the flow of negative charges. Further important is a high resistance against gas permeability and thermal resistivity.

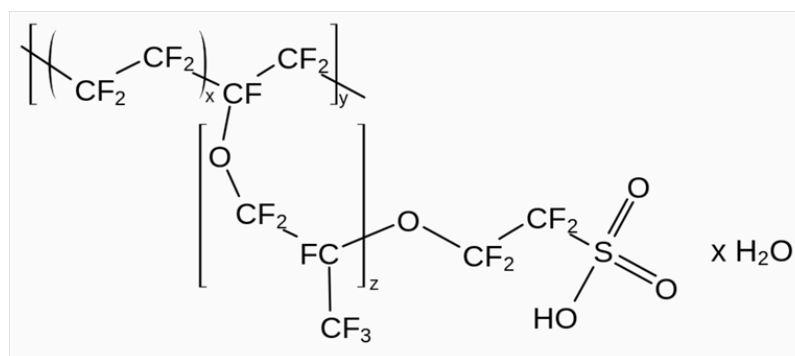


Figure 2.5: Chemical structural formula of Nafion® [6]

A far common material for low temperature PEMFCs is Nafion® from DuPont. The material stands out due to a high proton conductivity and high chemical stability.[6] The material is made of Polytetrafluoroethylene PTFE (Teflon) with integrated sulfonic acids (SO_3^- molecules). The SO_3^- molecules give Nafion® its quality to conduct protons when it is hydrated. The chemical structural formula is depicted by the illustration 2.5.

By the existence of water the membrane becomes moistened due to the polarity of the sulfonic acids. As side effects the volume and the mass of the membrane increase. H_2O accumulates to the SO_3^- groups and the PEM is now able to conduct protons while sufficient electron isolation is given due to the Teflon base. It would be optimal to reduce the thickness as much as possible due to the fall of the ionic resistance and a better water conduction. On the contrary the resistance to gas permeability would sink. However a diffusion of gases cannot always be prevented. At temperatures of more than $80^\circ C$, normal Nafion®, which is modeled in this thesis, starts to dehydrate and loses its capability to conduct protons.

2.1.5 Stack Design

Fuel cells are a promising candidate for the use in electric cars. A typical electric car needs a continuous power of about 60 kW. Since the typical operating voltage of a PEM fuel cell is lower than 1 V this would make a current flow of more than 60 000 A necessary. If only one fuel cell is used it must have an active area of more than $60\,000\text{ cm}^2$. A better option is to serially connect the cells in order to reach higher voltages and lower the current flow. The so combined cell pack is simply called fuel cell stack.[4]

The stack has to be supplied with the reaction gases and provision of gases is usually constructed in a way that every cell has the same pressure and species concentration at the gas channel entrances i.e. the supply principle is based on a parallel approach. In between the cells are the cooling channels. They are physically separated from the gas channels and are only responsible for temperature control.

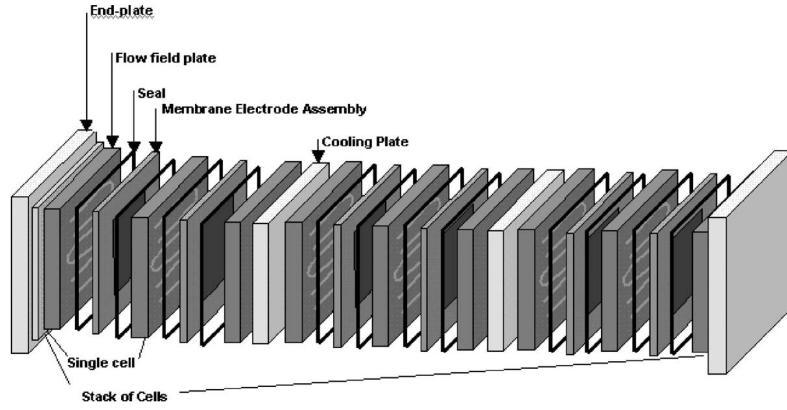


Figure 2.6: Stack architecture [7]

2.2 Physical Effects of a PEM Fuel Cell

This section is dedicated to the physical effects of the PEM fuel cell. As there are numerous different effects concerning operation of a cell, this section only gives an overview. The main physical effects can be distinguished in electrochemical, thermodynamic and fluid dynamic effects. Due to different time horizons of the several effects the dynamics of the cell is dominated by thermodynamics and fluid dynamics.

2.2.1 Thermodynamics

A fuel cell converts chemical energy directly into electrical energy while the whole process is far from perfect. Heat losses arise due to several imperfections which make it necessary to develop advanced control strategies for the operation of a cell or stack. The highest possible energy that can be transformed is the Gibbs free energy ΔG . If an open electric circuit is considered this is the highest reachable rate at given standard conditions.[8]

$$\Delta G = \Delta H - T\Delta S \quad (2.1)$$

The free Gibbs energy is calculated from the enthalpy difference of the individual reaction components ΔH reduced by the entropy difference $T\Delta S$ at a given temperature.

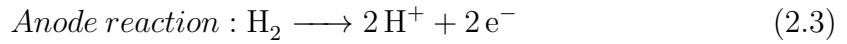
$$E_r = \frac{\Delta G}{nF} \quad (2.2)$$

It has to be distinguished if water appears in the liquid or gaseous phase at the end of the reaction. In the first case hydrogen's HHV (Higher Heating Value) is taken and

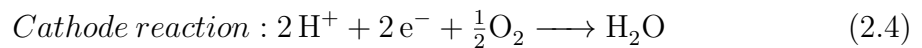
in the second case hydrogen's LHV (Lower Heating Value) because the water vapor has a higher enthalpy than in the liquid phase. In the PEM fuel cell the outgoing value is the HHV at 25°C and atmospheric pressure and the amount of energy that can be transformed into electricity is given by the Gibbs free energy. The Gibbs free energy changes with different temperatures and pressures and the maximum nominal voltage of the cell is calculated via equation (2.2).[4]

2.2.2 Electrochemicals

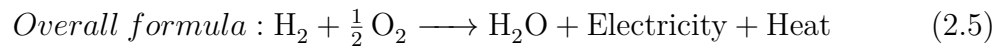
The fundamental electrochemical reactions take place in the CLs or more precisely at the three phase regions in the CLs. The formula for the anode is as follows:



Hydrogen oxidizes to protons and electrons. The presence of the catalyst material reduces the activation energy and the probability increases for the occurrence of the oxidization. To be more precise, a permanently splitting and recombination of the components take place which is described by the exchange current density. It is the reactivity of the electrode or can be interpreted as a kind of readiness of the electrode to continue with the reaction in one specific direction. The more reactive an electrode is the less energy is needed to precede with the reaction and the higher the cell efficiency. This dynamic has been described by Max Volmer with further development of John Alfred Valentine Butler and is simply called the Butler-Volmer Equation. It provides an interconnection between voltage losses, also called activation losses, and the net-current density in an electrochemical kinetic reaction.



Although the oxidation is a central physical process in a PEM fuel cell it is kinetically much faster than the cathode reaction, or reduction reaction, as all reactants are involved. The end-product of this process is clean water. The electrochemical reaction is described for both electrodes by the Butler-Volmer Equation which is treated in a separate section.



The products from the redox reaction are on the one hand water, electrical performance and waste heat. Heat losses appear by the chemical reactions and from the transport of charges. At some stage of cell operation a level is reached where the gases are not able to diffuse fast enough to the reaction site. The consequence is an

additional sharp drop of the cell operating voltage. These additional losses are called concentration losses.

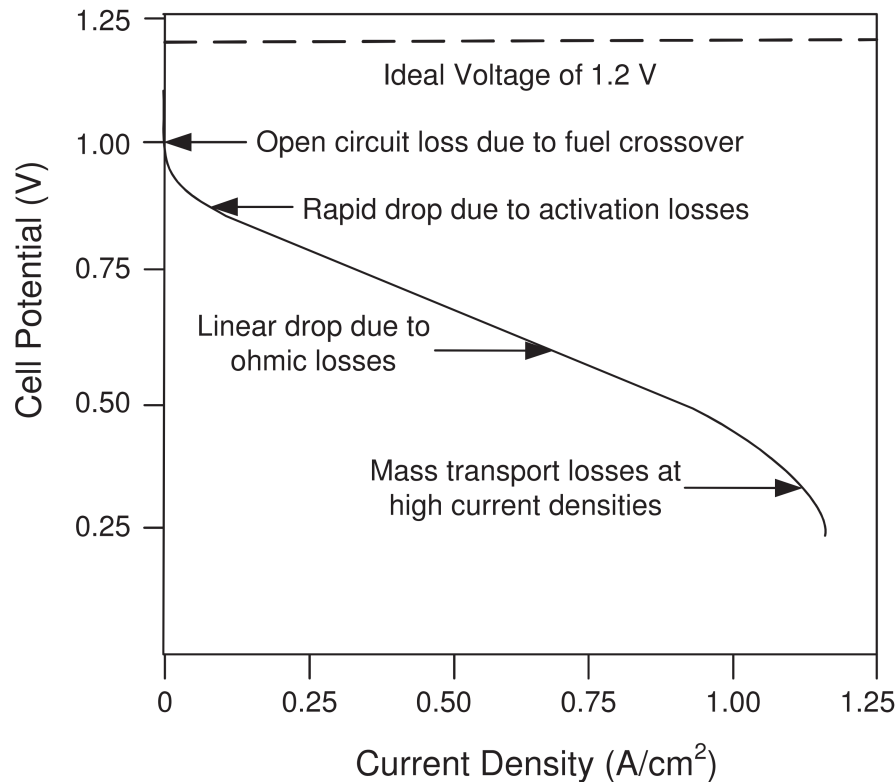


Figure 2.7: Polarization curve [8]

The development of the voltage-current characteristic of a PEM fuel cell, the polarization curve, is processed graphically in illustration 2.7. At the beginning stands a sharp drop caused by the activation losses of mainly the cathode electrode. The linear drop in the tension is characteristic for the middle segment for what mainly the charge transport losses are responsible. The final fall at the end of the curve is due to the concentration losses.

Charge Double Layer

The Charge Double Layer is a local load collection respectively at the boundary between the catalyst and the membrane layers. The reason why these local load collections occur is the different materials used. They cause a form of resistance for the charge transport and additional force in form of potential difference is needed to overcome the barrier. A potential distribution along the layers of a cell shows the illustration 2.8. At the anode the protons accumulate in the area of z_1 to z_2 and form a local potential difference. This effect has to be noticed also in the cathode in the area of z_3 to z_4 .

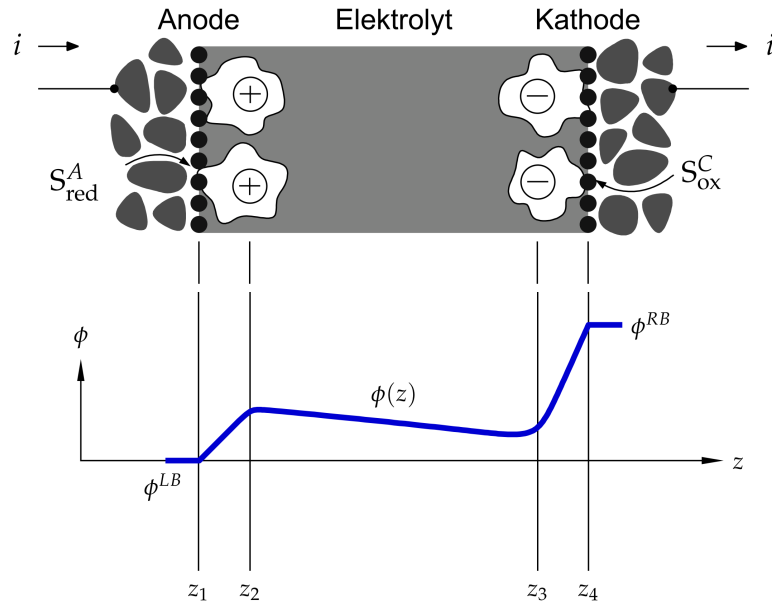


Figure 2.8: Charge double layer [9]

If now a step is applied to the cell the voltage falls strongly at the beginning. Then regenerates until the voltage has reached its stationary value. One recognizes a phase shift of the tension regarding the current. In the work of Pathapati [10] the transient behavior of a PEM fuel cell Stack is modeled. The characteristic effects occur after a step is applied to the model illustrated in figure 2.9 at second 600 and 1200. This behavior was modeled with the installation of a capacitor into the electrical circuit diagram.

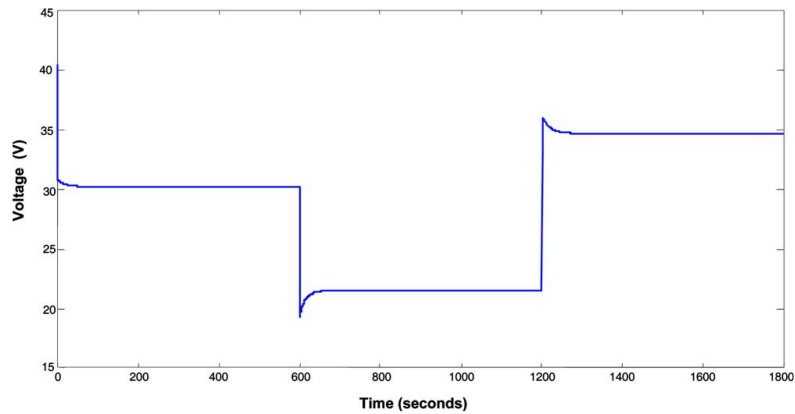


Figure 2.9: Phase lags due to the charge double layer [10]

2.2.3 Charge Transport

Flow of Electrons

Free electrons arise from the anode reaction. The potential difference between anode and cathode electrodes exerts a driving force on the charges found at the anode. Since the membrane works as an isolator for electrons they have to move through the electric energy consuming application. On its way they have to flow through the BPs where the gas channels are integrated. This leads to a problem where a compromise must be achieved between the area of gas channels and the charge conducting contact surface between BP and GDL. The ohmic resistance of all negative charge conducting materials shall contribute as little as possible to additional losses.

Transport of Protons through the PEM

The protons are able to conduct through the hydrated membrane. The conductivity of the membrane increases significantly with the water content. In fact the hydration of the membrane and the whole water management in the cell are crucial factors for the cell operation. Water management is treated in section 2.2.5.

The protons accumulate at the boundary layer between catalyst layer and membrane. They form the already treated Charge Double Layer. As of a certain point the force is so big on the protons that they can flow through the membrane. This process is not perfect and leads to further voltage losses, the ionic resistance losses. The strong dependency between water and conductivity is described by the ratio of H_2O to SO_3^- molecules, the water content. The higher the water content the lower the membrane resistance.

2.2.4 Gas Dynamics

The gas channels are used for the mass transport at anode and cathode side. Reaction gases are provided and the products and reaction gases not converted leave the cell at the end of the channel course again. Furthermore they can be actively used for cell temperature control if there is no active cooling of the stack. Several sources and sinks affect the mass balances on each side of the cell and regarding diffusion and convection of the several components the gas dynamics of PEM fuel cells is advanced to model. No limits are set to the imagination of the channel geometry design. Particularly important factors are: The flow resistance should be minimal and the membrane should be moistened as effectively as possible.

2.2.5 Water Management

A proper water management is crucial when operating a low temperature PEM fuel cell. The water management is considered as a highly challenging task and can be quoted as main disadvantage of this type of cell. A surplus of water in the cell leads to condensation drops in the porous media and the consequence is a disabled mass flow

of the reaction species which leads to a collapse of the stack operating voltage. On the other hand if there is less water available in the cell the membrane dries and the proton flow resistance increases dramatically. In order to prevent the cell from these from happening it is advantageous if the reaction gases can be moistened additionally. Furthermore an intelligent active cooling system allows the precise control of the cell temperature for ensuring mainly the optimal operating temperature.

2.2.6 Heat Losses

All upcoming cell losses arise in the form of heat. That is the energy part of hydrogen's HHV that cannot be transformed to electricity. Given standard conditions the theoretical maximum electrical degree of effectiveness of a PEM hydrogen fuel cell is calculated from hydrogen's HHV and is 1.482 V. The difference between the maximum voltage and the actual cell voltage, depending on the operational state, is the energy part that gets transformed into heat. Depending on the operational field of the system the heat can sometimes be used like in cars or stationary systems. The heat management is a crucial factor. If the temperature falls too deep then the amount of liquid water in the cell could dramatically increase which would lead to flooding of the cell. On the contrary, if the temperature rises over $\tilde{80}^{\circ}\text{C}$ the PEM loses its ability to conduct protons.

Chapter 3

Modeling a PEM Fuel Cell

A complete mathematical description of a PEM fuel cell requires 3D transportation equations. They describe the transient transition of physical volume attributes. This includes the density, the negative "electrical" or positive "ionic" charge, the energy, the impulse, the substance preservation and the pressure. The conservation equations have to be configured for every of the normally seven layers of a cell to model the different numerous physical phenomena. This is done by adding source and sink terms supplemented with proper boundary conditions.

Concerning the resources and the effects intended to reproduce, the modeling efforts have to be focused on the dominating behavior. Simplifications of the real system and the deletion of insignificant effects that do not have relevant influence on a global scale lower the modeling efforts to the desired scale. The model set up in this thesis is too an abbreviation of the general description.

The following chapter deals with the set of conservation equations and the boundary conditions. The work of Barbir [4] served as a reference. Further interpretations and exemplary judging tables for the parameters used here are found in [22, 23, 1].

3.1 Continuity equation

As a classic conservation equation it results from the differential form of Reynolds transportation theorem. It indicates that every change of the mass density occurs exclusively by a transportation of mass in or out of the volume. During the operation of hydrogen fuel cells, the ongoing chemical reactions process the transformation of mass. Mass defects do not appear inside the cell because the mass components only change their shape. The continuity equation is valid for the whole cell or for every cell layer.^{3.1}

$$\frac{\partial \rho}{\partial t} + \nabla \cdot (\rho \mathbf{v}) = 0 \quad (3.1)$$

The density ρ is related to the volume and does not distinguish between the individual mass types. \mathbf{v} is the velocity vector. The temporal change of the density is determined by the divergence of the mass current density $\rho\mathbf{v}$. The density can therefore be changed only with variations of $\rho\mathbf{v}$.

$$\nabla = \begin{pmatrix} \frac{\partial}{\partial x} \\ \frac{\partial}{\partial y} \\ \frac{\partial}{\partial z} \end{pmatrix}$$

$$\nabla \cdot = \left(\frac{\partial}{\partial x} + \frac{\partial}{\partial y} + \frac{\partial}{\partial z} \right)$$

Boundary Conditions and Source Terms

The supply of the cell with mass is only carried out via anode and cathode gas channels. The mass is transported to the cell and away to the ambient again. That is the only way mass can change if the whole cell is considered. In the cell the mass stream is composed of several types of species components but the mass conservation equation does not distinguish between the distinct mass types, just the mass itself is set to balance.

The materials of bipolar plates, gas diffusion layers and catalysts aren't subject to any change although in more advanced models, which contribute altering effects, it can occur that some insidious species stick to the cell. The volume of the membrane increases with a rising water content. The accumulation of water in the membrane is described with the diffusion laws after Fick.[24] Furthermore, at the three phase boundary in the catalyst layer mass is adsorbed by the platinum and protons are transported through the ionomer.

3.2 Momentum Conservation

The following equation is the momentum conservation equation 3.2 in the cell.

$$\frac{\partial \rho\mathbf{v}}{\partial t} + \nabla \cdot (\rho\mathbf{v}\mathbf{v}) = -\nabla p + \nabla \cdot (\mu_{eff} \nabla \mathbf{v}) + S_m \quad (3.2)$$

It is an expansion of the Euler equation for friction free flows. The change by time of the momentum density $\rho\mathbf{v}$ is on the one hand provided by its divergence $\nabla \cdot (\rho\mathbf{v}\mathbf{v})$ and on the other hand by the influence of surrounding forces. This would be body forces like the gravitational force or surface forces described by the remaining terms. These

are the pressure term $-\nabla p$ and on the one hand the tension of an incompressible flow $\nabla \cdot (\mu_{eff} \nabla \mathbf{v})$. Body forces are neglected and the source terms are treated in the following section.

Boundary Conditions and Source Terms

By the modeling of a flow field with friction the solution must be a steady distribution of the speed. Due to intermolecular forces the flow velocity vectors adapt to each other tangentially. Nearby walls it comes to adhesive forces between wall and fluid. The same applies to the modeling of the flow in the gas channels. Additional flow resistance must be taken into account in the porous layers. This is applied by the additional term S_m .

Gas channels:

In the gas channels no reactions occur. At one side of the gas channels the GDL is located and there the gases diffuse to the CL.

$$S_m = 0 \quad (3.3)$$

Diffusion and catalyst layers:

The porous character of the GDL and CL is taken into account via the additional term 3.4. This source term represents a pressure drop due to the flow of a medium through a porous material, Darcy's law. K is the permeability which links the penetration of the fluid directly to the concentration. ϵ describes the porosity itself and is calculated from the ratio of cavity volume to total volume. The parameter μ describes the mixture average viscosity, the resistance of a medium against the shear or tensile stress.

$$S_m = -\frac{\mu}{K} \epsilon v \quad (3.4)$$

Membrane:

The modeling of the water transport in the polymer layer requires the term 3.5. This term comprises the electrokinetic and the hydraulic permeability, K_ϕ and K_p .

$$S_m = -\frac{\mu}{K_p} \epsilon_m x_m v + \frac{K_\phi}{K_p} c_f n_f F \nabla \phi_m \quad (3.5)$$

3.3 Conservation of Energy

The temperature distribution through the cell is defined by the heat transport equation:

$$(\rho c_p)_{eff} \frac{\partial T}{\partial t} + (\rho c_p)_{eff} (\mathbf{v} \cdot \nabla T) = \nabla \cdot (k_{eff} \nabla T) + S_e \quad (3.6)$$

The heat transient is determined by the heat convection term $(\rho c_p)_{eff} (\mathbf{v} \cdot \nabla T)$ and the heat conduction $\nabla \cdot (k_{eff} \nabla T)$. c_p is the average specific heat capacity and " k_{eff} " the thermal conductivity. The source term S_e is dependent on the current cell layer. Heat arises from the transport of positive and negative charges and chemical reactions. In multiphase models sources from evaporation and condensation have a significant influence.

The subscript $_{eff}$ signals conditions of porous media. The solid phase is indicated by the subscript $_s$.

$$(\rho c_p)_{eff} = (1 - \epsilon) \rho_s c_{p,s} + \epsilon \rho c_p \quad (3.7)$$

The modification is carried out with the use of characteristic values of the solid phase. So e.g. the energy density per Kelvin ρc_p is adapted with the porosity factor ϵ . k_{eff} is adapted the same way. The membrane and the outer layers are not porous. Nevertheless, the equations of the gas diffusion and catalytic layers must be adapted.

$$k_{eff} = -2k_s + \left[\frac{\epsilon}{2k_s + k} + \frac{1 - \epsilon}{3K_s} \right]^{-1} \quad (3.8)$$

Boundary Conditions and Source Terms

In order to take into account the local heat gradients at the outer surfaces of the cell and in between the cell layers, the individual boundary conditions have to be formulated. The spring terms have different shapes depending on the modeling level.

Gas channels:

The only heat source in the gas channels is condensing or vaporizing water. Vaporizing water appears as a heat source if liquid water is available in the gas and the vapor pressure has not been reached yet. Condensation occurs if the gas is already saturated and the gas temperature drops. The expressions $x_{H_2O(g)}$ and x_{sat} stand for fraction of water vapor in dry gas and the maximum mass fraction of water vapor in dry gas. The rate of heat exchange during the evaporation is defined by the evaporation coefficient σ . Δh_{fg} is the heat of evaporation and A_{fg} is the change of the

surface area through the transition.

$$S_e = -\sigma A_{fg}(x_{sat} - x_{H_2O(g)})\Delta h_{fg} \quad (3.9)$$

The term 3.9 is at nonsaturated gas negative, i.e. a heat sink. It behaves differently if $x_{sat} < x_{H_2O(g)}$ is valid.

Diffusion layers:

Sources and sinks are determined out of two terms. On the one hand the evaporation and condensation term as described in last section. On the other hand the ohmic resistance term $\frac{i_e^2}{\kappa_{eff}^s}$. Electrons are separated in the catalytic layer and drain away over the bipolar layer. By passing through the diffusion layer they produce heat.

$$S_e = \frac{i_e^2}{\kappa_{eff}^s} - \sigma A_{fg}(x_{sat} - x_{H_2O(g)})\Delta h_{fg} \quad (3.10)$$

Catalytic layers:

The main heat sources are found in the catalyst layers. The chemical reactions appearing there are responsible for the main part of the heat production. On the right side in equation 3.11 the first term is derived from the activation overpotential ΔV_{act} and the creation of entropy $\frac{T\Delta S}{nF}$. The second term takes into account the dissipated heat resulting from the charge transport of electrons and protons. In addition, the condensation and evaporation enthalpy must be taken into account.

$$S_e = |j| \left[|\Delta V_{act}| - \frac{T\Delta S}{nF} \right] + \left(\frac{i_m^2}{\kappa_{effm}} + \frac{i_e^2}{\kappa_{effs}} \right) - \sigma A_{fg}(x_{sat} - x_{H_2O(g)})\Delta h_{fg} \quad (3.11)$$

Membrane:

Heat losses in the membrane are due to proton charge transport. The lower the water content level of the membrane the higher the heat losses. The expression κ_m cites the membrane conductivity for the protons in the ionomer.

$$S_e = \frac{i_m^2}{\kappa_m} \quad (3.12)$$

3.4 Conservation of Species

The calculation of the species concentrations determines the distribution of all the substances appearing in the cell. With this knowledge it is possible to determine local partial pressures, diffusion gradients or generally species distributions along the

gas channels.

$$\frac{\partial \epsilon \rho x_i}{\partial t} + \nabla \cdot (\mathbf{v} \epsilon \rho x_i) = \nabla \cdot (\rho D_i^{eff} \nabla x_i) + S_{s,i} \quad (3.13)$$

The transient $\frac{\partial \epsilon \rho x_i}{\partial t}$ is dependent from the temporal change of the mass fraction x_i . $i = 1, 2, \dots, N$ stands for the individual gas components (H_2 , O_2 , H_2O , ...) which can contain further gases appearing in air. Liquid water can be taken into account depending on the modeling detail. The term $\nabla \cdot (\rho D_i^{eff} \nabla x_i)$ represents the diffusion described after the law of Fick which relates the diffusive flux to concentration gradients. Therefore D_i^{eff} is the diffusion coefficient for a porous medium. The source term is treated in the next section.

Boundary conditions and source terms

The reactions treated hereinafter are described by the law of Faraday. In the catalytic layer of the anode H_2 is consumed and at the cathode O_2 is consumed or H_2O produced. The catalytic layers are the only region where chemical reactions occur. j_i is the current density and is treated in section 3.5.

$$S_{s,\text{H}_2} = -j_a \frac{M_{\text{H}_2}}{2F} \quad (3.14)$$

$$S_{s,\text{O}_2} = -j_c \frac{M_{\text{O}_2}}{4F} \quad (3.15)$$

Hydrogen and oxygen react to water and is computed with equation 3.16. Firstly, the product of the reaction is liquid water. Then the water vaporizes if the gas is still not saturated.

$$S_{s,\text{H}_2\text{O}(l)} = j_c \frac{M_{\text{H}_2\text{O}}}{2F} - \sigma A_{fg}(x_{sat} - x_{\text{H}_2\text{O}(g)}) \quad (3.16)$$

$$S_{s,\text{H}_2\text{O}(g)} = \sigma A_{fg}(x_{sat} - x_{\text{H}_2\text{O}(g)}) \quad (3.17)$$

3.5 Conservation of Charge

The last conservation equations are 3.18 and 3.19. They refer to the conservation of positive and negative charges. The outcome is the potential distribution throughout

the cell and by calculation the potential differences the cell voltages derive.

$$\nabla \cdot (k_s \nabla \Phi_s) = S_{\Phi_s} \quad (3.18)$$

$$\nabla \cdot (k_m \nabla \Phi_m) = S_{\Phi_m} \quad (3.19)$$

Φ_s and Φ_m are the potentials of the solid phase and the polymer depicted in V. The divergence of the charge flow is set equally with the source term S_{Φ_i} . The transient of the potential distribution is negligible and is not taken into account when it comes to charge conservation. k_i is the electrical conductivity in the polymer or solid matter.

Boundary Conditions and Source Terms

At the three phases region in the catalytic layers the reactants are produced. The several reactants are located in the three different phases i.e. the protons in the polymer, the electrons in the solid matter and the atomic oxygen is on the surface of the catalyst. The electrons move through the bipolar plate and the consumer to the cathode and react at the three phase border with oxygen and the protons to form the final product, water. The protons, therefore, move exclusively in the polymer.

The production of reactants is described by the Butler-Volmer equation. It connects the local tension difference $V_{act,i}$ with the electrochemical current j_i . An absolute necessary condition which must be fulfilled at all time is that the sum total of the produced charges at the anode is equal to all the used charges at the cathode. In addition the sum total of ionic charges is at all times equal to the electric charges, $|S_{\Phi_m}| = |S_{\Phi_s}|$ in every control volume.

$$j_a = ai_{0,a}^+ \left[\exp \left(\frac{-\alpha_a F \Delta V_{act,a}}{RT} \right) - \exp \left(\frac{(1 - \alpha_a) F \Delta V_{act,a}}{RT} \right) \right] \quad (3.20)$$

$$j_c = ai_{0,c}^+ \left[\exp \left(\frac{-\alpha_c F \Delta V_{act,c}}{RT} \right) - \exp \left(\frac{(1 - \alpha_c) F \Delta V_{act,c}}{RT} \right) \right] \quad (3.21)$$

j_i is the current density depicted in $A \cdot m^{-3}$. Negative and positive charges are produced at the anode, i.e. $S_{\Phi_m} = j_a$ and $S_{\Phi_s} = -j_a$. In contrast, the cathode where $S_{\Phi_m} = -j_c$ and $S_{\Phi_s} = j_c$ is valid. a is the electrocatalyst surface area per control volume in m^{-1} and $i_{0,i}^+$ is the exchange-current density per catalytic surface area in $A \cdot m^{-2}$.

The potential difference is calculated the following way.

1. The activation overvoltage as a local potential difference of polymer and solid

matter:

$$V_{act} = \Phi_s - \Phi_m - V_{ref} \quad (3.22)$$

2. The theoretical maximum cell potential:

If the partial pressures P_i near the catalyst layers are known, it is possible to model the concentration losses as well.

$$V_{ref} = - \left(\frac{\Delta H}{nF} - \frac{T\Delta S}{nF} \right) + \frac{RT}{nF} \ln \left[\left(\frac{P_{H_2}}{P_0} \right) \left(\frac{P_{O_2}}{P_0} \right)^{1/2} \right] \quad (3.23)$$

3. The cell potential:

The final cell potential is the difference between the two electrodes, the catalytic layers.

$$V_{cell} = \Phi_{s,c} - \Phi_{s,a} \quad (3.24)$$

3.6 Ideal Gas Law

The ideal gas law completes the system of equations. The temperatures and pressure conditions in a PEM fuel cell allow the assumption of an ideal gas mixture. The ideal gas law does not account molecular size and intermolecular interactions. The best fit is achieved with high temperatures and low pressures.

This was the general theory about the physics and the holistic modeling of PEM fuel cells. Chapter 4 now starts with the model concept treated in this thesis and how the general approach is simplified.

Chapter 4

Development of the Model Concept

The previous section has shown that a precise mathematical model of a PEM fuel cell requires several conservation equations, which are applied to seven or more layers. Such a model is highly sophisticated and is generally not capable of short simulation times by using standardized computational hardware. This chapter defines the model requirements and why the general mathematical model description was simplified.

4.1 Model Requirements

The main motivation was to create a PEM fuel cell Stack model which is capable of fulfilling several tasks and also offers short simulation times and a possibility to configure the model. The main requirements were short simulation times, comfortable configuration of the model and the operating environment of the model should be Matlab/Simulink. Furthermore, the model should offer the possibility of investigating gas concentrations. Then, at least a one-dimensional model with discrete gas channel elements is needed. The main reason why Matlab/Simulink was chosen as main operating environment is, because it can be easily linked together with other components like the BoPs, which provide the input information for the model.

During the development of the model concept, the possibility arose to work together with the AST department of the AVL company [25]. They explained how they currently model the after-treatment of catalytic exhaust gas systems with gas stream elements that are effected by catalytic reactions. As this is the same with a PEM fuel cell we developed the following modeling concept.

4.2 Model Concept

The idea was to create a model in BOOST RT by using existing components to model transient gas streams and temperatures. These elements are called Catalyst Core and Catalyst Substrate and together they simulate catalytic converters deployed

in exhaust systems. In order to get a full fuel cell stack model, a new, additional component had to be set up, namely the PEM Calculation Core, or PEM Core, which combines all the existing elements together and carries out the calculation of the remaining parameters linked with a fuel cell. These parameters are related to the modeling of electrochemical processes, the calculation of the heat and cooling power and the membrane-specific parameters, like ionic resistance and water content.

Figure 4.1 shows the model in BOOST RT just to give an idea of the structure. How the single blocks are configured is carried out in chapter 6.

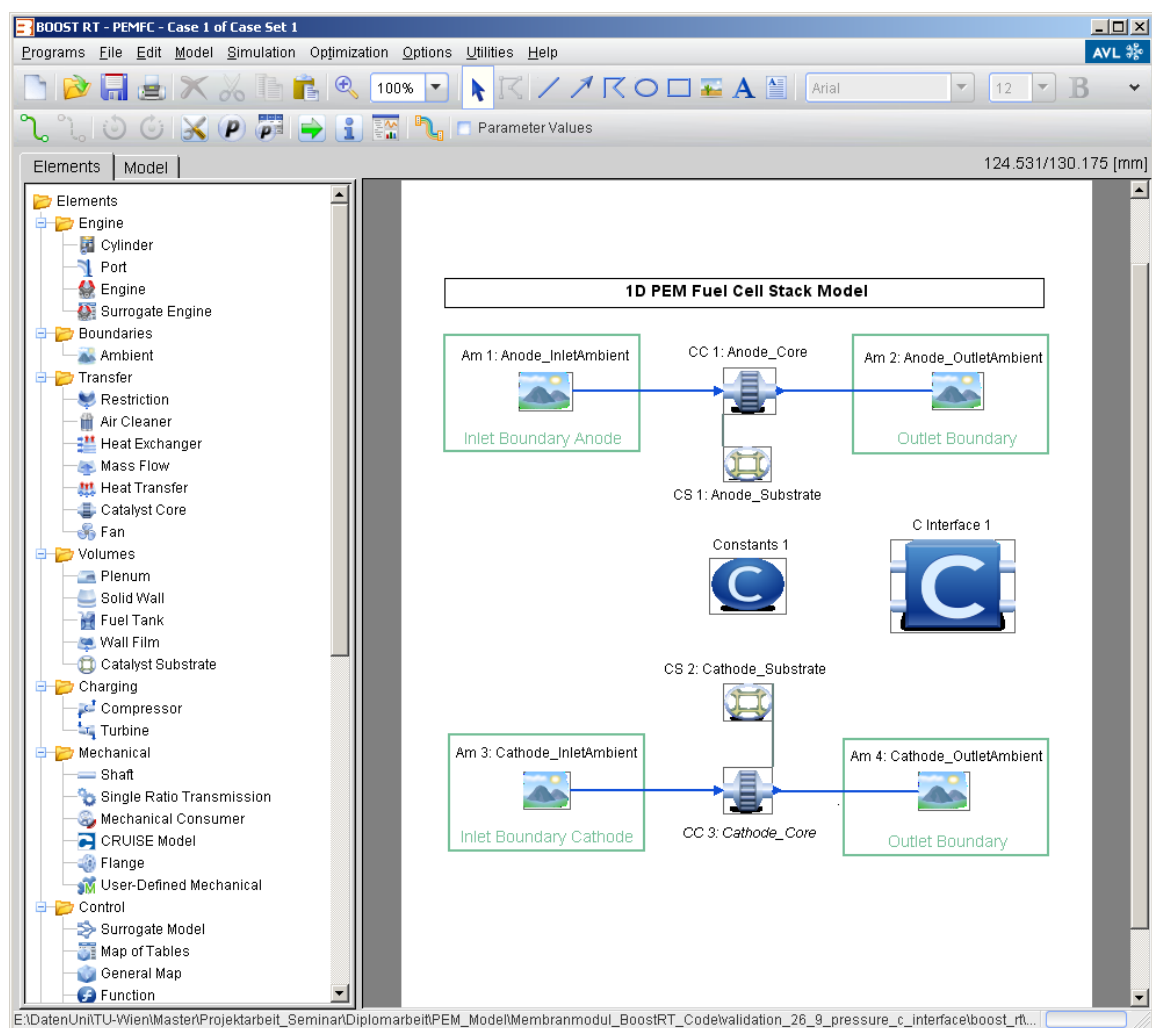


Figure 4.1: The BOOST RT PEM fuel cell stack model

In order to get channel specific data, we agreed on a one-dimensional model which is capable of simulating changing physical parameters concerning the whole PEM fuel cell along the gas flow channels. Another point was the possibility of interlinking

BOOST RT with Matlab/Simulink through a C-Interface. With the use of these existing elements it was possible to simulate transient gas and heat convection through both channels, namely the cathode and anode channel. The stack is then built up of several PEM Cells. They are serially connected to increase the system's operating voltage. The cell itself is made up of discrete cell elements where all elements are parallelly connected.

To sum up, this model is a discrete, one dimensional (along the channel), semi-empirical, transient gas and static electrochemical PEM fuel cell Stack Model.

4.2.1 The Simulation Environment BOOST RT

The following description of BOOST RT is derived from the AVL Product Description [26]. BOOST RT is a simulation tool that offers capabilities related to the real-time simulation of engines and the investigation of transient operating conditions. Its main functions are simulating gas streams through several types of engine components and thermal simulations which can be supplemented with mechanical components. Additionally, it offers components for control network functions, PID controllers and interfaces that interconnect BOOST RT to other types of programs. The simulation in Simulink does not require to run BOOST RT additionally. Only the calculation core of the program is started during the iterations. After that the results are issued in the form of an output vector.

4.2.2 The PEM Calculation Core encoded in C-Code

The existing components are now interconnected via data buses with an additional PEM Calculation Core that is encoded in C-Code. The PEM Core uses the data buses to get physical input data from the Catalyst Core and the Catalyst Substrate and delivers specified output data. Via the Catalyst Substrate the discretization of the channel is carried out and all the physical variables are evaluated for every cell element. How the complete model works and how the algorithm of the new part is structured, will be treated in the next chapter.

4.3 The Model Capabilities

The PEM fuel cell Stack model developed in this thesis is a 1D model for the anode and the cathode gas channels. Both gas channels and the PEM are discretized and simulated, which offers the possibility of investigating several physical parameters of the cell e.g. current densities, temperatures, gas concentrations and several more. The model can be operated via Matlab/Simulink and is able to reach a Real Time Factor of one or lower, depending on the boundary conditions.

The model is not able of simulating dynamic changes in the PEM fuel cell specific parameters. As far as the gas flow specific parameters are concerned, they are simulated

by the Catalyst Core which is capable of reproducing dynamic gas behavior. Furthermore, as the gases flow in a parallel direction the model can only simulate parallel flow channels. It's possible, however, to simulate a counter flow direction of the gases.

The overall model specifications are comprised in the table below:

Type of Specification	Description
Model dimension	One dimensional
Model operating environment	BOOST RT developed by AVL List GmbH
Additional operating environment	Matlab/Simulink
Channel Discretization	Yes, anode and cathode gas channel and the PEM
Modeled effects regarding the PEM	Water diffusion, drag effect, heat transportation through the membrane, transportation of hydrogen to the cathode
Modeled effects regarding the gas channels	Transient gas stream, sink and source terms for hydrogen, oxygen and water, heat sources, active cooling, cooling effects of gases
Appearing gas phases	The model does not distinguish between different gas phases
Flow field	Parallel flow of the gases but counter direction possible

The operation of the model should be carried out via a C-interface from Simulink. The model is configured in BOOST RT, where the Parameters are adapted and a calibration is carried out. The simulation in Simulink does not require running BOOST RT additionally. Only the calculation core of the program is started during the iterations. After that, the results are issued in the form of an output vector. However, the exact instructions are treated in chapter 6.

In the next chapter the reduced mathematical model is described and it is demonstrated how the components simulate the physical phenomena.

Chapter 5

The PEM Fuel Cell Model in BOOST RT

The precise mathematical model of a PEM fuel cell had to be simplified to establish faster simulations and easier configuration procedures. The key task was to find a balance between processing speed and precision. What the basic model concept looks like was previously discussed. In this chapter the precise equations are explained and which assumptions had to be made to combine the PEM Core with the Catalyst Core and Catalyst Substrate. The chapter is structured according to the different sub models for the electrochemistry, the thermal effects and the gas stream physics. The equations described in this chapter are encoded in the PEM Core and they are configured respectively. The model configuration and operation will be discussed in the chapter 6.

5.1 The Electrochemical Model in BOOST RT

The electrochemistry describes the species turnover and how the polarization curve of the fuel cell develops. Therefore the connection between voltage and the current density is the main physical law of a PEM fuel cell. This means that the model establishes the polarization curve along the discrete cell elements. Depending on several physical boundary conditions, the characteristic of the polarization curve changes at every discrete cell element, which leads to different performances and species turnovers. The performance of a cell is derived by multiplying the voltage with the current. A cell element is one discrete part of the cell.

5.1.1 Theoretical Voltage

The theoretical voltage, also the Nernst potential, describes the highest possible energy part of hydrogen's HHV (Higher Heating Value) which can be transformed into electricity. It can be measured between the two electrodes if the electrodes are not interconnected. It is influenced mainly by the partial pressures of the reactant species and the cell temperature. At operating temperatures less than 100°C, some simpli-

fications can be assumed.

The equation begins with the nominal voltage under standard operating conditions (1 bar, 25°C) which is 1,229 [V]. Depending on predominant temperature and pressure conditions, the nominal voltage is corrected. Although the Gibbs energy is dependent on temperature changes due to variations of dS and dH they are negligible at temperatures less than 100°C.[4] The realized Nernst potential can finally be calculated with equation (5.1).

$$V_{ref} = 1.229 - 8.45 \cdot 10^{-4} \cdot (T_{element} - 298.15) + 4.21 \cdot 10^{-5} \cdot T_{element} \cdot \ln(P_{H_2} \cdot P_{O_2}^{0.5}) \quad (5.1)$$

V_{ref} ... Highest cell potential at hydrogens LHV, Nernst potential, V

$T_{element}$... Average cell temperature, K

P_{H_2} ... Partial pressure of hydrogen, Pa

P_{O_2} ... Partial pressure of oxygen, Pa

5.1.2 The Implementation of the Butler-Volmer Equation

Basically, the Butler Volmer equation is defined for catalytic reactions at both electrodes of the cell. As the heat generation or the voltage losses due to the anode reaction can be neglected [27], only the activation losses at the cathode side are considered. A potential loss at the catalytic layers occurs because the ongoing reaction at the catalyst layer has to be forced in one direction. Therefore the basic rule can be explained as follows: the higher the current density, the more voltage has to be "sacrificed". One important condition is that all the produced charges at the anode side must be equal to the consumption of charges at the cathode side. This means that the amount of charge flow is equal at both sides of the cell. Equation (5.2) shows how the activation losses are calculated.

$$V_{act} = \frac{R \cdot T_{element}}{\alpha \cdot F} \cdot \ln\left(\frac{i_{element}}{i_0}\right) \quad (5.2)$$

V_{act} ... Activation polarization, V

R ... Ideal gas constant, J·kg⁻¹·K⁻¹

α ... Transfer coefficient at the cathode

F ... Faraday constant, C·mol⁻¹

$i_{element}$... Current density, $A \cdot m^{-2}$

i_0 ... Exchange current density at the cathode, $A \cdot m^{-2}$

Primarily the strong voltage drop of the polarization curve at low current densities can be explained by the activation overvoltage. Its dominance deteriorates at higher current densities. The exchange current density is a key factor for the performance of the fuel cell and is necessary to calculate the changes in the current densities when it comes to different pressure and temperature conditions. The pressure dependency can be varied but only in the code itself, where its standard value is 0.5. Finally i_0 is derived via equation 5.3.

$$i_0 = i_0^{ref} \left(\frac{P_r}{P_r^{ref}} \right)^\gamma \exp \left[-\frac{E_c}{RT} \left(1 - \frac{T}{T_{ref}} \right) \right] \quad (5.3)$$

i_0^{ref} ... Reference exchange current density at reference-pressure and -temperature, $A \cdot m^{-2}$

E_c ... Activation energy, $66 \text{ kJ} \cdot \text{mol}^{-1}$

P_r ... Partial pressure of oxygen, Pa

P_r^{ref} ... Reference pressure, 101 250 Pa

γ ... Pressure dependency coefficient, $0.5 - 1$

T ... Temperature, K

T_{ref} ... Reference temperature, 298.15 K

Equations (5.2) and (5.3) combined together now determine the voltage losses due to the catalytic reactions in the cell element at the cathode.

5.1.3 Ohmic and Ionic Losses

The ohmic and ionic losses are due to the resistance of materials against the flow of charges. Losses arise by the flow of electrons through the cell, which are the ohmic losses. The ohmic resistance constant R_{ohm} can be assumed as it is derived from the construction of the cell and the conductive material. Both attributes do not change during the simulation.

The far more important factor, though, is the constricted flow of protons through the proton exchange membrane. These losses are described with the ionic resistance constant R_{ion} , which underlies significant changes during the simulation because it mainly depends on the humidity degree of the membrane. The membrane ionic resistance is a key factor when it comes to modeling PEM fuel cells.

$$V_{ohm} = R_{ohm} \cdot i_{element} \quad (5.4)$$

V_{ohm} ... Ohmic voltage loss, V

R_{ohm} ... Ohmic resistance constant, $\text{Ohm} \cdot \text{m}^{-2}$

Ohm's law is used in order to describe the losses from the charge transport of electrons. Ohm's resistance is, therefore, known or one has to find a suitable value with a calibration method.

$$V_{ion} = R_{membran} \cdot i_{element} \quad (5.5)$$

V_{ion} ... Ionic voltage losses, V

R_{ion} ... Ionic resistance of the membrane, $\text{Ohm} \cdot \text{m}^{-2}$

The overall charge transport losses arise then from the sum total of the individual losses.

Membrane Model

The performance of the cell is influenced decisively by the qualities of the membrane. Especially when it comes to modeling the fuel cell dynamics, the physical behavior of the membrane dominates all the other effects.

The membrane model implemented is related to the work of Springer et al. [28]. The approach builds on experimental tests and has been used in numerous previous PEM models. The basic concept is the connection between water activity and water content through a membrane. The dynamics, though, cannot be reflected because the model uses measurements of the static water content in the membrane. With the knowledge of the water content the electric conductivity is calculated and from there the ionic resistance of the membrane. Further calculations regard the diffusion of water through the membrane as well as an overall description of the water transport due to the Drag effect.

The equations start with the water activity which can be approximated by the relative humidity ϕ . If an ideal gas mixture is assumed, which is the case in this model, it can be approximated as the ratio of partial pressure to equilibrium vapor pressure of water vapor. The code calculates the water activity for the anode and cathode

gas channel respectively. With knowledge of the water activity one can estimate the amount of liquid water in the channel. Since the model does not distinguish between different phases, this value is a main indicator to determine the water conditions. The gas specifications permit water to be in the gaseous phase up to the equilibrium vapor pressure. At higher pressures the water appears in the liquid phase. Nevertheless, water drops can arise in the porous layers also under the equilibrium vapor pressure and thus restrain the gas flow through the GDL. The model realized here, however, is not able to cope with this phenomenon.

$$\phi = \frac{P_{\text{H}_2\text{O}}}{P_{\text{H}_2\text{Osat}}} \quad (5.6)$$

ϕ ... Water activity or relative humidity

$P_{\text{H}_2\text{O}}$... Water partial pressure, Pa

$P_{\text{H}_2\text{Osat}}$... Equilibrium vapor pressure, Pa

The saturation pressure has to be calculated and depends solely on the temperature. With the empirical coefficients listed below the equation is valid within a temperature of 0°C and 100°C.[4]

$$P_{\text{H}_2\text{Osat}} = \exp \left[a \cdot T^{-1} + b + c \cdot T + d \cdot T^2 + e \cdot T^3 + f \cdot \ln(T) \right] \quad (5.7)$$

$$a = -5800.2206$$

$$b = 1.3914993$$

$$c = -0.048640239$$

$$d = 0.41764768 \cdot 10^{-4}$$

$$e = -0.14452093 \cdot 10^{-7}$$

$$f = 6.5459673$$

The next method computes the water content λ . From the determination of the water activities at anode and the cathode gas channels the level of the water activity through the membrane is linearly approximated. Now the membrane is discretized in the PEM Core and for every discrete membrane element the water content is calculated via equation (5.8) with respect to the domain of the function. At water activities higher than $a > 3$, the water content is set to the highest possible value which is 18.2.

$$\lambda = \begin{cases} 0.043 + 17.81 \cdot a - 39.85 \cdot a^2 + 36.0 \cdot a^3, & \text{für } 0 < a \leq 1 \\ 14 + 1.4 \cdot a, & \text{für } 1 < a \leq 3 \end{cases} \quad (5.8)$$

λ ... Water content

With the knowledge of the characteristic water content evolution in the membrane, the ionic conductivity σ can be calculated. Therefore equation (5.9) is encoded.

With the final equation (5.10) the resistance against the flow of ionic charges, the so called ionic resistance is derived. This is done for every cell element by integrating the inverse value of the ionic conductivity.

$$\sigma = (0.005139 \cdot \lambda - 0.00326) \cdot \exp \left[1268 \left(\frac{1}{303} - \frac{1}{T_{element}} \right) \right] \cdot 10^2 \quad (5.9)$$

$$R_{membran} = \int_0^{dm} \frac{1}{\sigma(\lambda, T_{element})} dz \quad (5.10)$$

$R_{membran}$... Total ionic resistance of the membrane element, Ohm·m²

σ ... Ionic conductivity, Ohm⁻¹·m⁻¹

dm ... Membrane thickness, m

The water content significantly influences the ionic resistance and the performance of the whole PEM fuel cell. As a consequence, a suitable humidity level is essential for the operation of the fuel cell stack. Two effects influence the water content in the membrane, namely the diffusion of water due to concentration gradients and the Drag effect. Among others, the Drag effect is determined from the electro-osmotic Drag coefficient. An approximation depending on the water content was published by Zawodzinski [29].

In the work of Spiegel [8] one recognizes after dissolving in discrete sections that no essential deviations of the water content arise due to the relatively low membrane strength. Since the membrane has no dimension the Drag effect N_{drag} is calculated with an average water content through the membrane. Water can only be transported from the anode to the cathode side because the hydronium ions H_3O^+ are dragged to the cathode side. Additionally the actual water drag on the anode side is the same as on the cathode side, it is only negative, which ensures the conservation of mass in the membrane.

$$n_{drag} = 2.5 \cdot \frac{\lambda}{22} \quad (5.11)$$

$$N_{drag} = n_{drag} \cdot \frac{i_{element}}{F} \quad (5.12)$$

n_{drag} ... Electro-osmotic Drag coefficient

N_{drag} ... Water transport due to the Drag effect, $\text{mol} \cdot \text{s}^{-1} \cdot \text{m}^{-2}$

The diffusion effect $N_{diffusion}$, though, can force water to flux in both directions. It depends on the gradient of the water content through the membrane. Since the conservation of mass has to be ensured, the water diffusion calculated at a current time step of a membrane element is supposed to be the same on both sides of the membrane, just the sign is different.

$$D_{membran} = (2.563 - 0.33 \cdot \lambda + 0.0264 \cdot \lambda^2 - 0.000671 \cdot \lambda^3) \cdot 10^{-10} \cdot \exp \left[2416 \cdot \left(\frac{1}{303} - \frac{1}{T_{element}} \right) \right] \quad (5.13)$$

$$N_{diffusion} = -\frac{\rho}{M_m} \cdot D_{membran} \cdot \frac{d\lambda}{dz} \quad (5.14)$$

$D_{membran}$... Membrane diffusion coefficient, $\text{m}^2 \cdot \text{s}^{-1}$

$N_{diffusion}$... Water diffusion, $\text{mol}^2 \cdot \text{s}^{-1} \cdot \text{m}^{-2}$

ρ ... Density of the dry membrane material, $\text{kg} \cdot \text{m}^{-3}$

M_m ... Molecular weight of the membrane, $\text{kg} \cdot \text{mol}$

The diffusion gradient is the key factor for calculating the diffusion through the membrane. A sufficient approximation of the diffusion gradient provides equation (5.15).

$$\frac{d\lambda}{dz} \approx \frac{\lambda_c - \lambda_a}{dm} \quad (5.15)$$

This was the calculation of the main factors regarding the membrane. With the ohmic and ionic resistance together, the resistance against charge flow has been considered and is mainly responsible for the linear fall in the mid section of the polarization

curve. Also the transport of water through the membrane has been described which is a key factor regarding the water management of a PEM fuel cell.

The sharp drop in the last section of the polarization curve is mainly due to concentration losses, which are comprised in section 5.1.4.

5.1.4 Concentration Losses

Concentration losses result due to the fact that the performance limit of the catalyst is reached. It is not possible to sustain the supply of reactant gasses as fast as it would be necessary. In a reduced model these losses must be considered with the use of diffusion resistances or with a correction factor. The following empirical equation serves as a reference and was published by Kim et al. [30]. The concentration losses are fitted by optimizing the empirical coefficients c and d .

$$V_{conc} = c \cdot \exp\left(\frac{i_{element}}{d}\right) \quad (5.16)$$

V_{conc} ... Concentration voltage losses, V

c ... Empirical coefficient, V

d ... Empirical coefficient, $A \cdot m^{-2}$

To this point the activation polarization, ohmic plus ionic and the concentration losses have been encoded. As these are the main components of the voltage losses the polarization curve can be developed.

5.1.5 Cell Potential

The main part of the model, the polarization curve, can be developed by calculating the relation of the current density to the cell voltage. Equation (5.17) shows that the cell potential $V_{element}$ is the Nernst potential minus the sum total of all voltage losses. To be able to find a solution for this problem either the cell potential or the current density have to be given. In consultation with the AVL List GmbH the conclusion was made that the voltage can be considered as constant value among all cell elements and the current density is variable.

Equation (5.17) together with the information of a constant cell voltage among the cell channel is now evaluated by a numerical solver that finds the correct current density for every cell element. This solution depends on all the previously discussed voltage losses and the current density can change significantly along the cell channel with different physical conditions. The final current is derived by multiplying the current density with the reactive cell area A_{reac} . The individual currents are

summed up and the result is the total current of one cell related to the actual given cell voltage.

$$V_{element} = V_{ref} - V_{ohm} - V_{ion} - V_{conc} \quad (5.17)$$

To sum up, $V_{element}$ is the realized cell potential under operating conditions and is equal in all cell elements. Variations concern all other components. In the model the solution, which is the current density, is calculated with the use of a zero point search function. This happens for every single cell element. Then the currents of all cell elements are summed up which leads to the total current of one cell. The stack is usually build up of serially connected cells, as it is the case in this model, and the final stack current is the same as the cell current.

$$i_{stack} = i_{cell} = \sum i_{element} \cdot A_{reac.element} \quad (5.18)$$

$$V_{stack} = V_{element} \cdot \#zellen \quad (5.19)$$

- $A_{reac.element}$... Reactive cell area per cell element m^2
- i_{stack} ... Stack current, A
- i_{cell} ... Cell current, A
- V_{stack} ... Stack potential, V
- $\#_{cell}$... Number of cells in the stack

This was the electrochemical model in BOOST RT. The next section describes the thermal model and the simulation of the gas and species model is comprised in section 5.3.

5.2 The Thermal Model in BOOST RT

The thermal model calculates the temperature changes of the fuel cell due to the waste heat and the active cooling of the system. The operating temperature of a fuel cell is correlated to the PEM because the functional principle of the fuel cell depends decisively on the attributes of the membrane. A very common membrane material for low temperature PEMFCs is Nafion[®]. Most of the claims to a PEM are met by Nafion[®] but the important feature to conduct protons gets lost at a temperature of approximately 100°C. Consequently, the optimal operating temperature of a PEM hydrogen fuel cell lies in an area of 75°C. This temperature should be sustained

throughout the operation of the stack which can be influenced by the construction of the cooling system.

Generally the algorithm of the thermal model can be explained as follows. At the beginning the heat generation of every cell element is calculated. Therefore, all the potential losses are transformed into heat and appear as heat sources in the Catalyst Substrate element. The cooling power of every cell element is calculated out of the temperature difference between the average cooling fluid temperature and the average cell temperature which is the same as the stack temperature. This overall cell cooling power is equally distributed to the single cell elements which appear as cooling source terms in the Catalyst Substrate. The temperature changes of each cell element are calculated via the Catalyst Substrate which takes into account the temperature effects of the gasses too. Finally the PEM Core evaluates the impact of the cooling power to the cooling fluid outlet temperature with the knowledge of the the cooling fluid mass stream and the cooling fluid inlet temperature.

5.2.1 Cell Potential with Hydrogen's HHV

The HHV of hydrogen is the amount of energy released if all of the hydrogen is burned and the products are allowed to cool down to 25°C. In a fuel cell a part of this energy is converted to electricity. Due to the fact that the reaction releases entropy, heat is generated and the arising loss, or the fuel cell heat production, is calculated from the difference of the theoretical cell potential regarding hydrogen's HHV and the cell potential under operating conditions. The maximum theoretical cell potential regarding hydrogen's HHV (Higher Heating Value) is also dependent on the temperature and the predominant pressure conditions and is equal to (5.1) except of the first entry. At the beginning, V_{HHV} is calculated for every cell element.

$$V_{HHV} = 1.482 - 8.45 \cdot 10^4 \cdot (T_{element} - 298.15) + 4.21 \cdot 10^{-5} \cdot T_{element} \cdot \ln(P_{H_2} \cdot P_{O_2}^{0.5}) \quad (5.20)$$

V_{HHV} ... Theoretical cell potential regarding Hydrogens HHV, V

The next sections treat the calculation of the heat which is generated during the operation of fuel cell and the cooling power due to the parameters of the cooling system.

5.2.2 Fuel Cell Heat Generation

The heat power $Q_{reac.element}$ generated during the operation of a fuel cell is calculated for every cell element. The difference between V_{HHV} and the cell potential $V_{element}$ is multiplied by the current of each cell element. The result is the reaction heat power per cell element.

$$\dot{Q}_{\text{reac.element}} = (V_{HHV} - V_{\text{element}}) \cdot i_{\text{element}} \quad (5.21)$$

The sum total of heat power of all cell elements multiplied by the number of cells in the stack is the total reaction heat power.

$$\dot{Q}_{\text{reac}} = (\sum \dot{Q}_{\text{reac.element}}) \cdot \#_{\text{cells}} \quad (5.22)$$

Depending on the operating state and stack construction, sufficient cooling power can be achieved just by the exchange of reactant gases. However, the regulation of the membrane humidity gets more advanced without a separate active cooling system.

5.2.3 Cooling Power of the Active Cooling System

Active cooling is necessary at certain dimensions of a stack depending on the stack construction. The big advantage is the enhanced stack temperature control. The cooling power \dot{Q}_{cool} refers to the cooling power for the overall stack. The cooling power is determined by the surface of all cooling channels inside the stack, the heat-transfer coefficient between streaming coolant and cell element and the driving temperature gradient. As cooling fluid temperature the average temperature is chosen. The final cooling power of the stack is scaled down to every cell element and is implemented as cooling term in the Catalyst Substrate.

$$\dot{Q}_{\text{cool}} = A_{\text{cool.channel}} \cdot \alpha_{\text{cool}} \cdot (T_{\text{stack}} - \frac{T_{\text{cool.in}} + T_{\text{cool.out}}}{2}) \quad (5.23)$$

\dot{Q}_{cool} ... Cooling power for the stack, W

$A_{\text{cool.channel}}$... Inner surface of the cooling channels, m²

α_{cool} ... Cell current, W·m⁻²·K⁻¹

T_{stack} ... Stack average temperature, V

$T_{\text{cool.in}}, T_{\text{cool.out}}$... Temperature of the cooling fluid in and outlet, K

The heat transfer coefficient is a crucial factor for the effectiveness of the cooling system and is derived from the Nusselt number Nu . The Nusselt number is dimensionless and establishes a relation between heat conduction with stationary and moving contact surfaces. The Nusselt number is significant for the calculation of the heat transfer and the main variable factor when it comes to the fitting of the cooling system. The characteristic length L_{kanal} is the length of the overflowed area and can

be denoted as diameter of one cooling channel.

$$\alpha_{cool} = \left(\frac{Nu \cdot \lambda_{fluid}}{L_{kanal}} \right) \quad (5.24)$$

Nu ... Nusselt number

λ_{fluid} ... Heat conductivity of the fluid, $\text{W} \cdot \text{m}^{-1} \cdot \text{K}^{-1}$

L_{kanal} ... Characteristic length of the cooling channel, m

The next section describes how the temperature of the stack or cell and the cooling fluid is calculated.

5.2.4 Calculation of Temperature Changes

With the knowledge of the reaction heat and the cooling power the temperature change in every cell element is carried out by the Catalyst Substrate depending on the stack material. The definition of the stack material is done via the BOOST RT GUI, which is treated in a later chapter. In addition, a thermal interaction between reaction gases and solid matter is considered. As the temperature is evaluated for every cell element an average value for the cell temperature is used and the cell temperature is equal to the stack temperature.

The control of the cooling power is carried out with the coolant mass flow \dot{m} or by changing the coolant initial temperature. Depending on the cooling fluid heat capacity the cooling fluid exit temperature $T_{cooling.out}$ rises or falls, according to the stack temperature.

$$T_{cool.out} = \frac{\dot{Q}_{cool}}{\dot{m} \cdot c_{fluid}} + T_{cool.in} \quad (5.25)$$

c_{fluid} ... Cooling fluid heat capacity, $\text{J} \cdot \text{kg}^{-1} \cdot \text{K}^{-1}$

This was the basic calculation procedure regarding the thermal model. The last main modeling domain is the simulation of the gas stream channels which is comprised in section 5.3.

5.2.5 The Catalyst Substrate

The Catalyst Substrate is an element which is available in the BOOST RT environment. With the Catalyst Substrate the thermal calculations of the solid material surrounding the gas channels is carried out. Which kind of material is used can be defined in the BOOST RT GUI. The sink and source terms are added to the code of the Catalyst Substrate and effect the temperature of the solid. This is also true for the sink and source terms regarding the species changes.

Furthermore the discretization is done via this element and the user can define the amount of discretization points. Nevertheless, the transient simulations done in the Catalyst Core are not affected by the discretization. The Catalyst Core reads the data at discrete points of the Catalyst Core and the PEM Core assumes now that the cell is divided in the discrete sections.

5.3 Modeling of the Gas Channels

The gas stream is simulated via the second key component previously available in BOOST RT, the Catalyst Core. Depending on the boundary conditions at the gas channels entry a stream develops which is influenced by the catalytic reactions in the Catalyst Substrate. Later in the work it is shown that the user can decide if a mass flow-driven configuration is desired or the pressure boundary conditions are provided and the proper gas stream will establish depending on the friction flow coefficients.

5.3.1 Species Turnover

The gas stream is affected by the species turnover in every cell element. H_2 is reduced at the anode side of the cell and transported to the cathode side. There O_2 is reduced and finally H_2O is produced. The species turnover is calculated by using Faraday's law of electrolysis which links the quantity of mass reduced by electrolysis directly to the quantity of electric charges produced at the electrode.

$$N_{O_2.element} = -\frac{i_{element}}{4 \cdot F} \quad (5.26)$$

$$N_{H_2.element} = -\frac{i_{element}}{2 \cdot F} \quad (5.27)$$

$$N_{H_2O.element} = \frac{i_{element}}{2 \cdot F} \quad (5.28)$$

$$N_{O_2.element} = \text{Oxygen turnover per cell element, mol}\cdot\text{s}^{-1}$$

$$N_{H_2.element} = \text{Hydrogen turnover per cell element, mol}\cdot\text{s}^{-1}$$

$$N_{\text{H}_2\text{O},\text{element}} = \text{Water production per cell element, mol}\cdot\text{s}^{-1}$$

Furthermore the drag and diffusion effects transport water through the membrane and appear as water sink or source terms in the Catalyst Substrate. The difference is that these effects just transport water whereas the terms in this section reduce or produce the substance of matter. They have already been defined in equations (5.12) and (5.14).

5.3.2 The Catalyst Core

The Catalyst Core is the central element when it comes to the simulation of the gas streams and again two are used to simulate the anode and the cathode gas channels. The main responsibility of this element is the transient gas stream simulation through a drilled holed solid. The number and shape of the drill holes are defined in the GUI. In addition the predefined laminar and tabular gas flow friction coefficients can be either changed itself or adapted via a friction multiplier.

Together with the Catalyst Substrate the gas streams of the anode and cathode are modeled. The gas flows towards a drilled holed surface and through the channels towards the outlet. While they pass through the channels the source and sink terms influence the mass balance.

5.4 The C-Code Calculation Kernel or PEM Core

The C-Code calculation kernel, or the PEM Core, is the main calculation core where all the parameters are combined and the PEM fuel cell specific parameters are evaluated. Via data buses all the necessary information is available from the Catalyst Core and the Catalyst Substrate. This information is then used to calculate all the cell related parameters.

The calculation kernel consists of two files, namely the “brt_pemfc.h” and “brt_pemfc.c”. The first file is the header file and comprises the declaration of all the data and variables used in the code. Furthermore, it defines the results which are saved during the simulation and can be investigated afterwards. The difference between data and variables is that data values stay constant over the simulation. These would be parameters which regard the physical dimensions of the cell or fitting parameters like the ohmic resistance. In contrast stand the variables which change over the simulation cycle.

The source code is comprised in the “brt_pemfc.c” file. The main structure is the “operate_pemfc” method which calls all the algebraic equations in a predefined order. The algebraic equations have been discussed previously in this chapter. They are encoded as methods in the source code and can be called by the “operate_pemfc”

method. For a better clarity most of the methods are standardized in its structure which is declaration, initialization and then the equation. Of course not all of the methods can be structured as simple as that but for most of them this would be the case.

The PEM Core can be configured via the Constants element. The data buses of the PEM Core are attached via the Data Bus Connections. Therefore the Anode Core link has been adapted in a way that all the data buses of the PEM Core can be linked to the Constants element except of CELL Potential, COOLANT Massflow and COOLANT Temperature In. This data has to be provided via the C-Interface which would come from Matlab/Simulink or the user can change the connections. Then the information is given by some other components like a function. Figure 5.1 shows the connections of the additional PEM Core input data. Figure 5.2 shows the output data of the PEM Core which can be linked to other components via the Anode Substrate link.

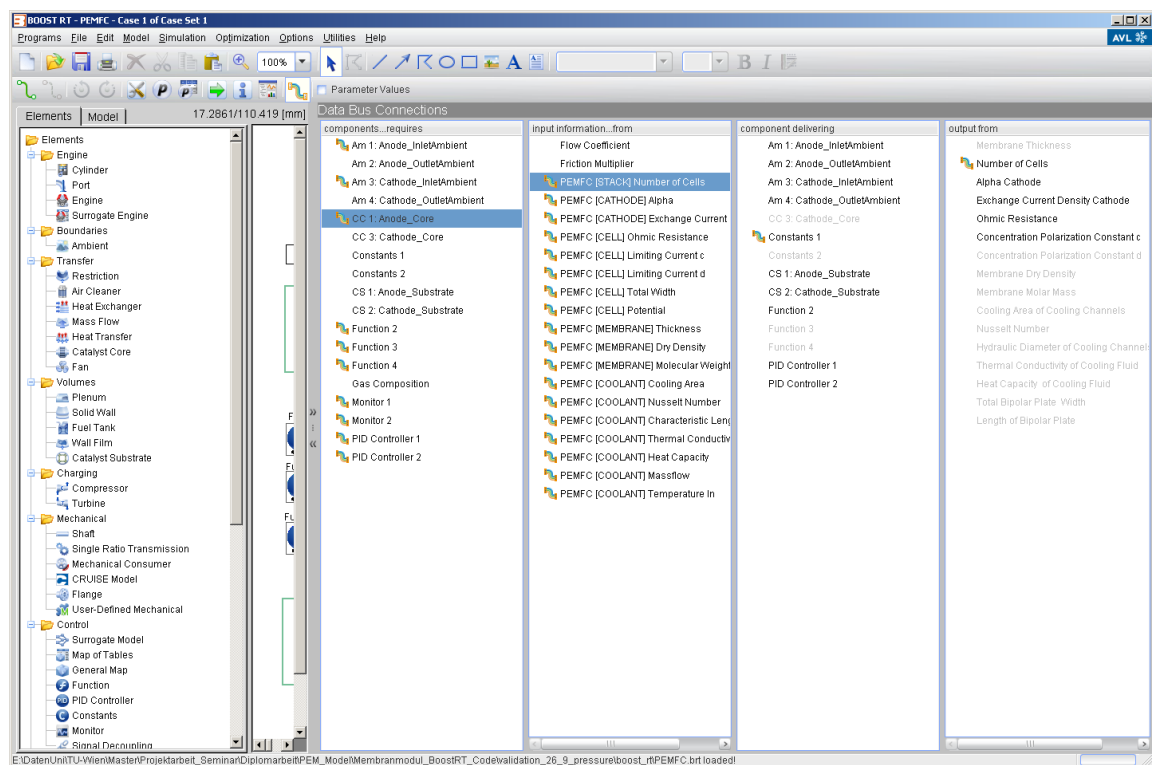


Figure 5.1: Additional PEM Catalyst Core data buses

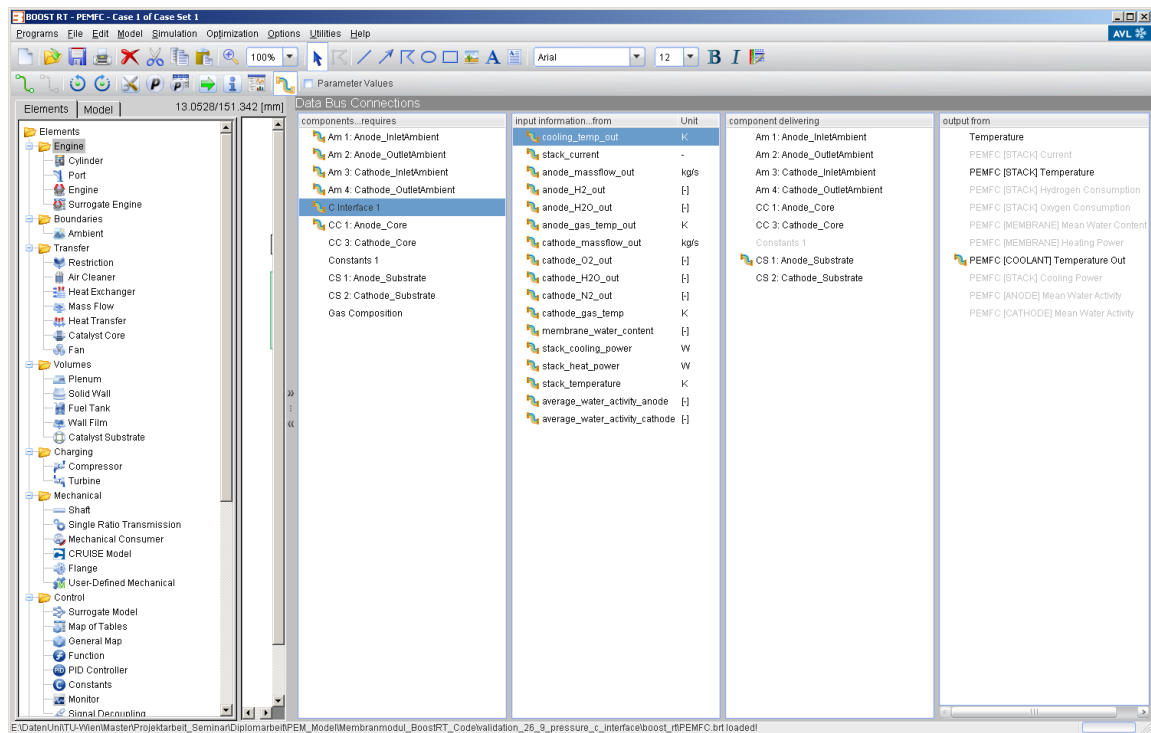


Figure 5.2: PEM Catalyst Core output data

The calculation core is called at every cell element. So the algorithm starts at the first cell element and runs through the calculations. Then it starts again with the next cell element until all elements have been calculated. Then the Catalyst Core and Catalyst Substrate execute their calculations.

Chapter 6

Model Configuration and Validation

This chapter comprises the general preparation and use of the model. It shows the adaptations of the BOOST RT installation and some further adaptations which have to be done to link BOOST RT with the PEM fuel cell model. It shows the different kinds of the model configurations and the procedure of how the model is finally linked to Matlab/Simulink.

If the general part leaves some questions unanswered then continue with the second and third part of this chapter. They comprise the configuration and validation of a real PEM fuel cell. This system is reproduced in the BOOST RT model and most of the general configuration procedures are executed. Then the simulation results are compared to the measurements of the experiment.

The last part of the chapter summarizes all the outcomes.

6.1 General Configuration of BOOST RT, -Program and -Model

6.1.1 General Preparation of BOOST RT

The operational platform of the PEM fuel cell model is BOOST RT (v2011.2), a program from the AVL List GmbH. The correct version of BOOST RT is necessary for the model to run. After installing the correct version, proceed with the following adaptations to the installation:

First of all, copy the “element_data” file into the directory “AWS/v2011.2/python/clients/boost_rt/res” located in the installation file of BOOST RT. Then make a save copy of the original file. The aim of the “element_data” file is to configurate the data buses between BOOST RT and the C-Code calculation kernel.

Even though the model can be run solely in Matlab/Simulink, the model itself needs the BOOST RT kernel in order to run the calculations. The program needs to know where the membrane model is implemented. Therefore start BOOST RT and open the PEMFC.brt file. Choose the option “Options Environment Settings” on the command line of BOOST RT and enter the path to the application “MSVS_PEMFC/pemfc_brt/Release/pemfc_brt.exe” and be sure to cut out the “#” sign at the front of the line and to use Slash signs in the address path. The yellow box in the picture below shows the place where to put the path.

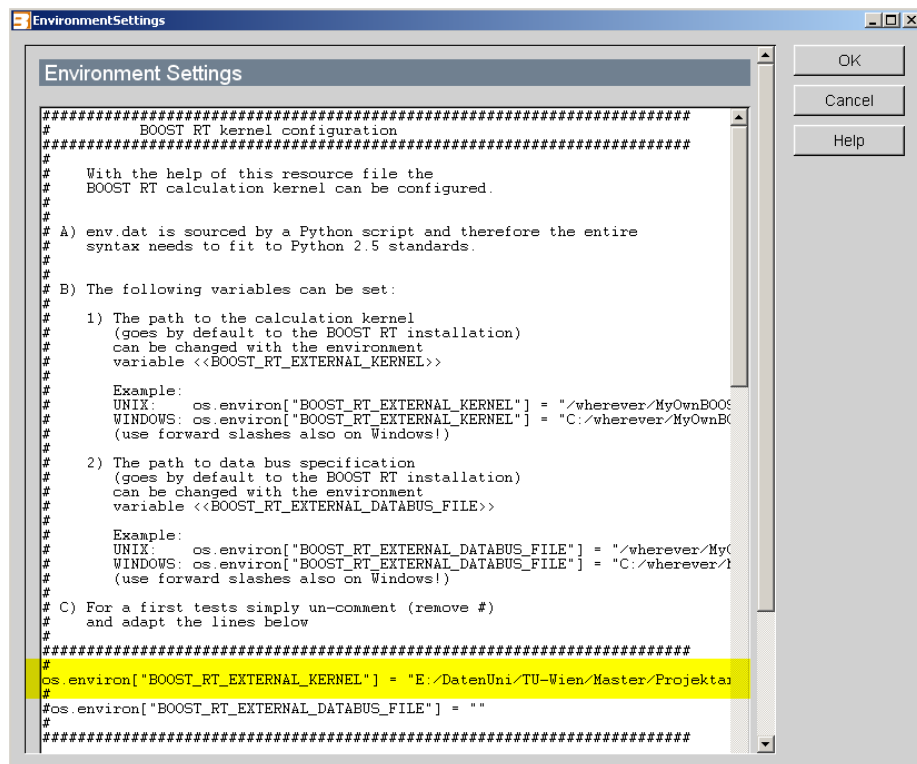


Figure 6.1: Configuration of the kernel

This was the basic procedure of preparing the program itself. The next step is to choose the model parameters according to a given stack or simply one PEM cell.

6.1.2 General Model Configuration

After having installed and adapted BOOST RT, the user can start to adapt the model parameters depending on the real PEM fuel cell stack. The model can be configured completely in the BOOST RT GUI. That is also true for the C-Code calculation kernel, which is configured via the Constants 1 element. The parameters are adapted, depending on the fuel cell stack. Therefore all the necessary data has to be prepared. If the information about the system is not available or incomplete, the

parameters have to be calculated or estimated. Here a general description is made of the configuration procedure. An example is given in the next section.

The first step is to decide whether the model is mass flow- or pressure-driven. If the pressure boundary conditions are provided a proper mass flow will result and, vice versa, if the mass flow is given, a proper pressure drop will result. To switch between the configurations just add/move the modeling blocks like shown in the figures 6.2 and 6.3.

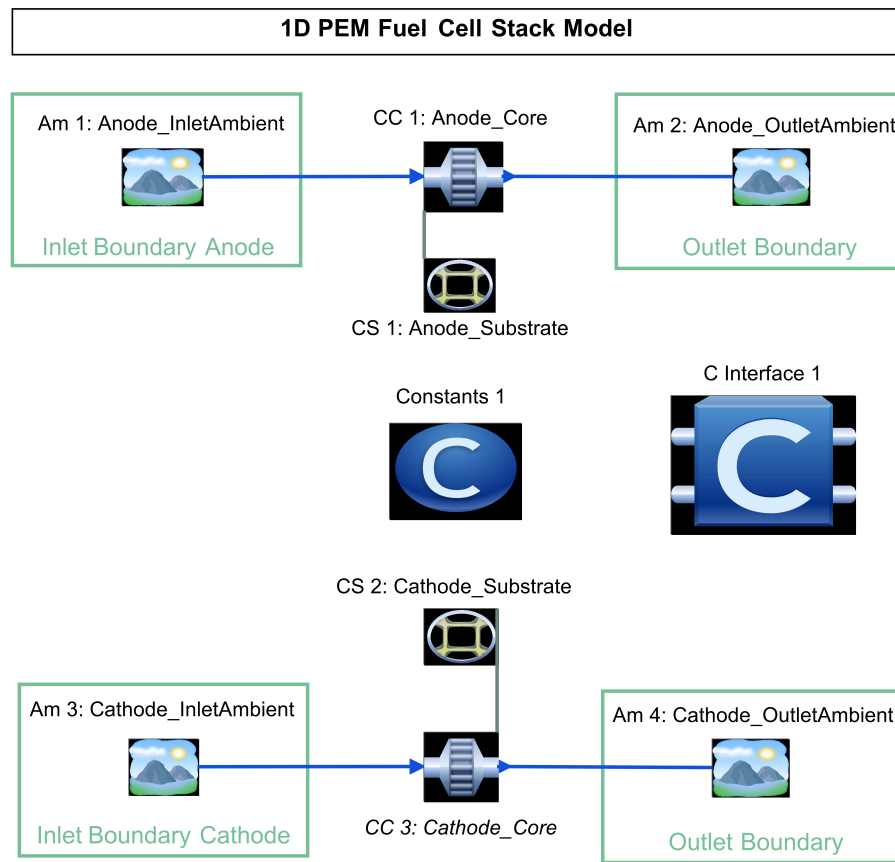


Figure 6.2: Pressure driven model configuration

Both figures show a parallel gas flow in equal direction but a simulation of a counter flow direction is possible too. Therefore just switch the ambient inlet element with the outlet element on the anode or cathode side. An example of a counter flow configuration is later shown in the validation example.

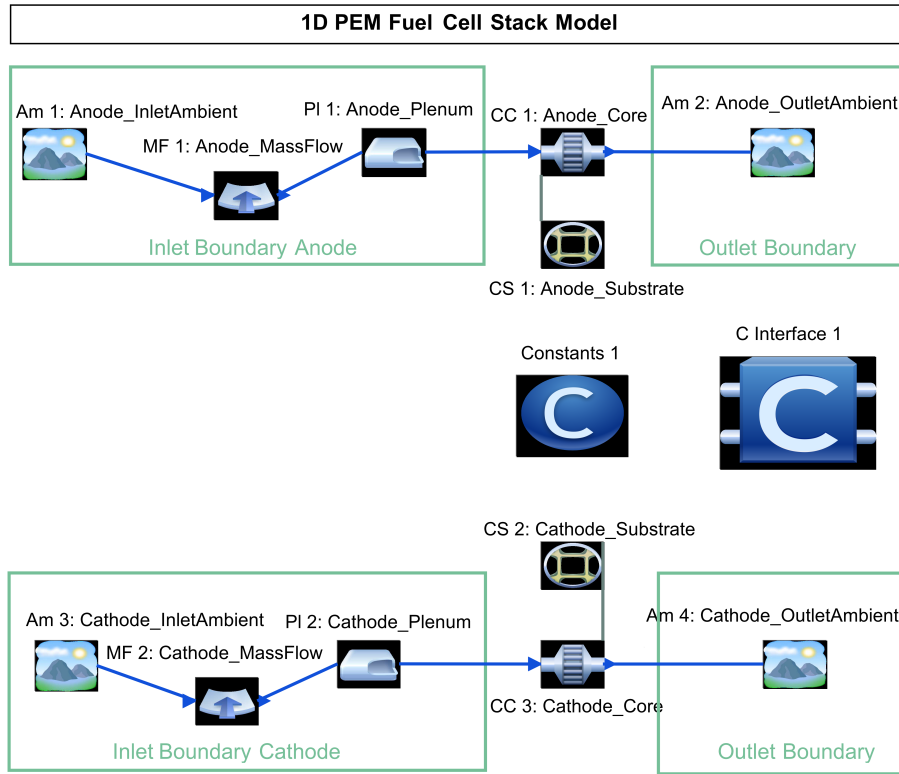


Figure 6.3: Mass flow driven model configuration

Then the appearing gases have to be adapted. They are generally configured for a standard simulation case where the basic gas components appear. These are H_2 , O_2 , N_2 , H_2O and the composition is shown in “Model → Gas Composition → General Species Transport “. If the user wants to extend the gas composition, he/she just has to add additional gas components by using the GUI. It is important to list all the species appearing in the gas stream because only pre-defined gases appear in the Ambient elements and can be used for the species composition.

The model is divided into two sections, the anode and cathode section. The Substrate elements simulate the physical effects of the solid, or, more precisely, only the heat effects and resulting temperature of the solid. It is not capable of distinguishing between the different materials that make up a cell. As the Catalyst Core element starts with the simulation of gas which streams to a drilled surface, the model has to be configured according to the actual conditions in the cell. So later in the configuration process another adaptation has to be done regarding the material. At this point an average material has to be defined which will be close to the physical parameters of the bipolar plate as it is basically the dominant layer. The material is defined in “Model → Solid/Fluid Properties - Used in Model “. As a standard material Graphite is used. The user can adapt the properties or create a new material.

The next step is the configuration of the BOOST RT elements. At the beginning

the Inlet Ambients are adjusted. There the gas pressure, gas temperature and the mass fractions of the species composition at the boundaries - i.e. the gas channels in- and outlets - are defined. The species that can be used in the Ambient elements were previously defined in the Gas Composition. The mass fractions of the species compositions must be at all time equal to one. Normally all the data is provided via the C-Interface from Simulink but if no data is available the Ambient takes the data from its own input fields. If the model is mass flow-driven, the mass flow is chosen and a constant pressure is defined in the Ambient elements. In figure 6.4 the anode Ambient input fields are shown. As far as the output Ambients are concerned, they do not affect the simulation, but they do affect the pressure distribution in the gas channels. The outlet species mass fractions and gas temperatures are provided by the Catalyst Core elements.

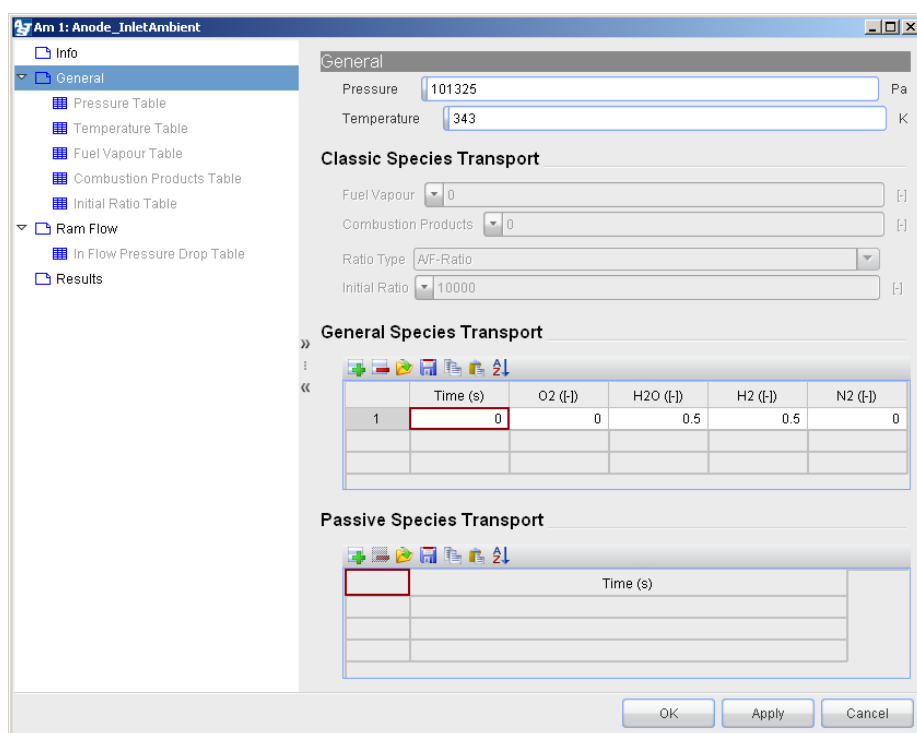


Figure 6.4: Anode Inlet Ambient

The geometry of the stack is modeled via the Catalyst Core elements. Figure 6.5 shows the GUI of the Catalyst Core filled with random values. As there are two Catalyst Core elements one simulates the anode and one the cathode. First of all, the length of the gas channels is defined. If the gas channel design is different from parallelly arranged channels, an average channel length should be chosen.

Secondly, the volumes Vol_{anode} and $Vol_{cathode}$ of the anode and cathode side of the cell are determined. Consequently, one Catalyst Core element is responsible for one

side of the cell. As the Catalyst Core elements simulate gas streams which flow towards an area of equally distributed drill-holes, the flow conditions in front of the gas channels have to be defined. Depending on the open frontal area a pressure loss is calculated by the Catalyst Core. The open frontal area is the proportion of the open surface to the total surface towards which the gas is streaming. So use a volume where the actual physical frontal area of the gas channels is multiplied by the length of the channels.

The next value is the Hydraulic Diameter depicted via equation 6.1. The variables w_c and h_c refer to the channel width and height.

$$D_h = -\frac{2w_ch_c}{w_c + h_c} \quad (6.1)$$

The Open Frontal Area OFA is a value that sets the open area at the front of the gas channel entry side $\sum A_{open}$ in contrast to the gas channel total frontal surface A_{total} .

$$OFA = \frac{\sum A_{open}}{A_{total}} \quad (6.2)$$

The last parameter is the Geometrical Surface Area GSA . It is the inner surface of all gas channels divided by the cell total volume which has been defined before.

$$GSA = \frac{\sum S_g}{Vol_{anode,cathode}} \quad (6.3)$$

There are further options that basically define the friction of gas flow in the channels. It is the user's choice to adapt these parameters too but the existing ones are empirically well-chosen. When the gas stream velocity and the pressure loss are fitted to the measurements the best way to adapt the gas flow friction is to change the Friction Multiplier, which can be adjusted externally.

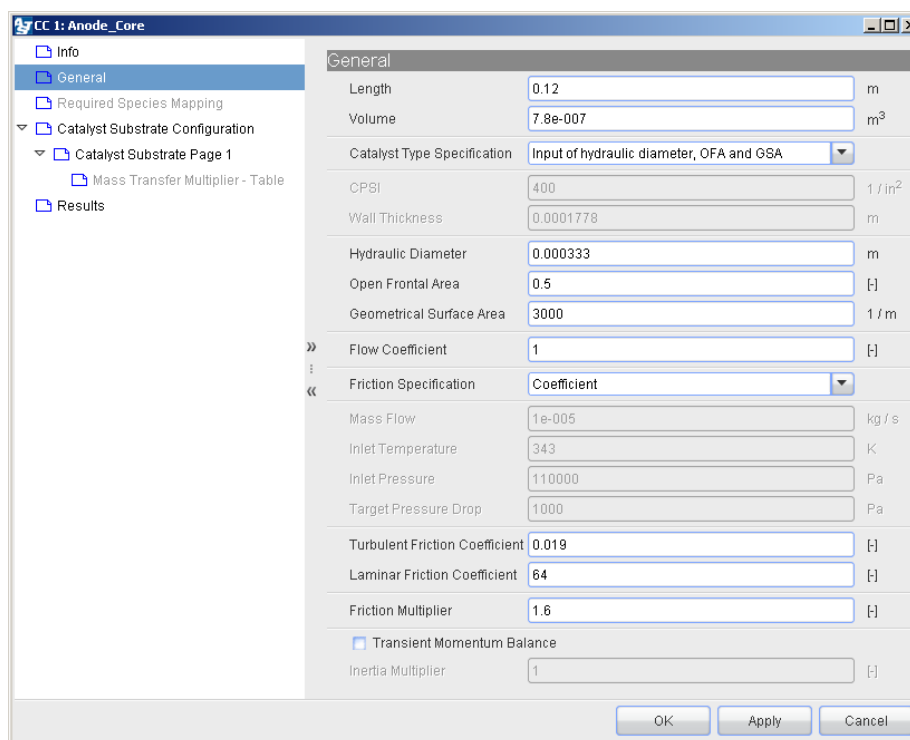


Figure 6.5: Catalyst Core element

The next key element is the Substrate. Again there are two of them which simulate anode and cathode separately. They are responsible for calculating the thermodynamics of the solid and the discretization of the channel is defined in its GUI.

The first entry regards the Washcoat Thickness. The Washcoat is a porous layer around the gas channel that absorbs gas species and the chemical reactions are located in this part. Basically, as it has a porous character, the Washcoat could be seen as comparable to a GDL but the Washcoat material surrounds the channel and the reactions start at the beginning of the layer. A GDL, by contrast, is only at one side of the gas channel and the reactions occur at the end of the layer. So the thickness of the Washcoat is chosen thinner than the actual GDL would be.

If the Axial Discretization is chosen, the Substrate element calculates discrete gas channel elements. The previously defined length of the channel is divided in equally distributed sections and the physical parameters are evaluated for every section. With the Grid Shape Factor them equal distribution could be changed into an unequal one but the model is not capable of different section sizes. Therefore, the Grid Shape Factor needs to stay at one.

The Initial Temperature is the temperature of the solid at the start of the simulation and in the last selection the material is chosen which has been predefined. Basically the material properties are defined for Graphite but the user has to change the material-specific coefficients in the Option “Model → Solid/Fluid Properties -

Used in Model“to meet the cell heat capacity. Therefore just multiply the average heat capacity with the stack cell volume and divide it by the two volumes of the anode and cathode Catalyst Core. Then change the heat capacity according to the result of this calculation.

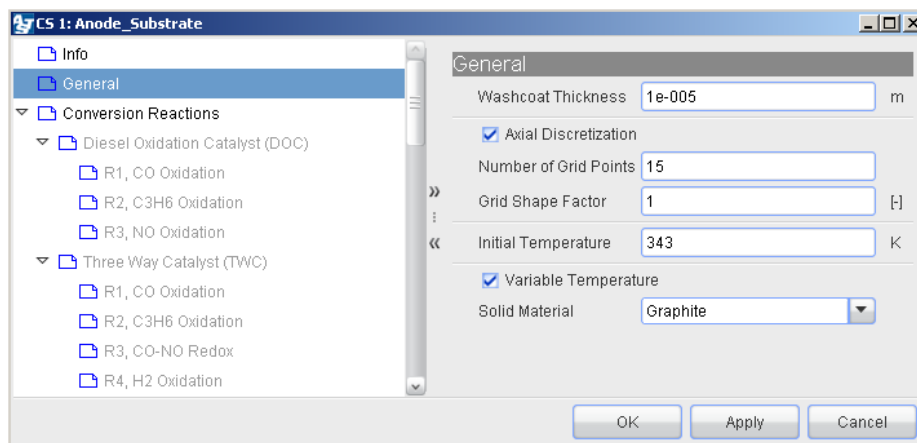


Figure 6.6: Catalyst Substrate element

The C-Code calculation kernel is configured via the Constants 1 element. All the remaining parameters are configured here and they are used for the electrochemical and the cooling model. The constants were described in previous sections. Figure 6.7 shows the GUI of the Constants 1 element.

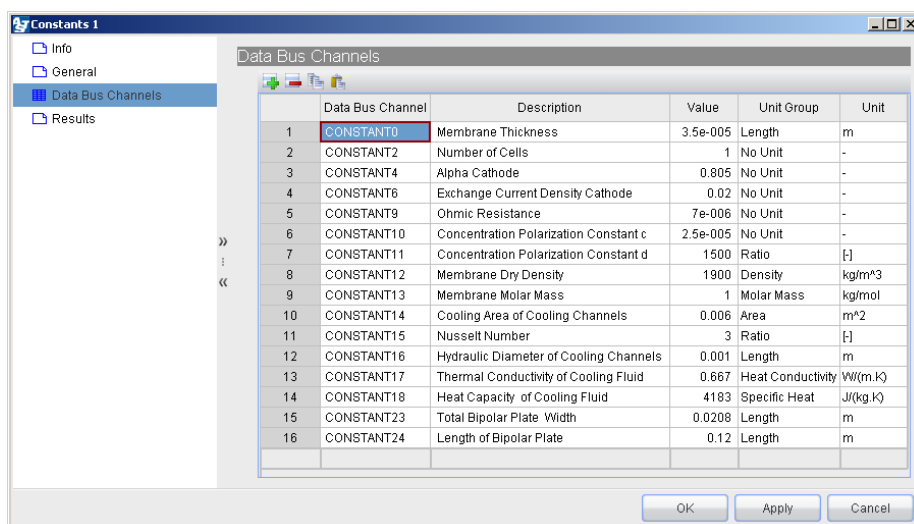


Figure 6.7: Constants element

Via the Data Bus Connections button in the BOOST RT GUI the input output con-

nections are set. By choosing the Data Bus Connections button the interface opens. The left two columns show the elements which can be provided with input information and the right two columns list the elements which can provide the data. Only when the physical units of input and output port are equal, a connection can be set up. The input output information is usually provided by the C-Interface. Therefore all the input output buses have to be defined in the C-Interface block. Take care of the fact that a C-Interface Inport is information that goes to Simulink and the Outport is data that comes from Simulink.

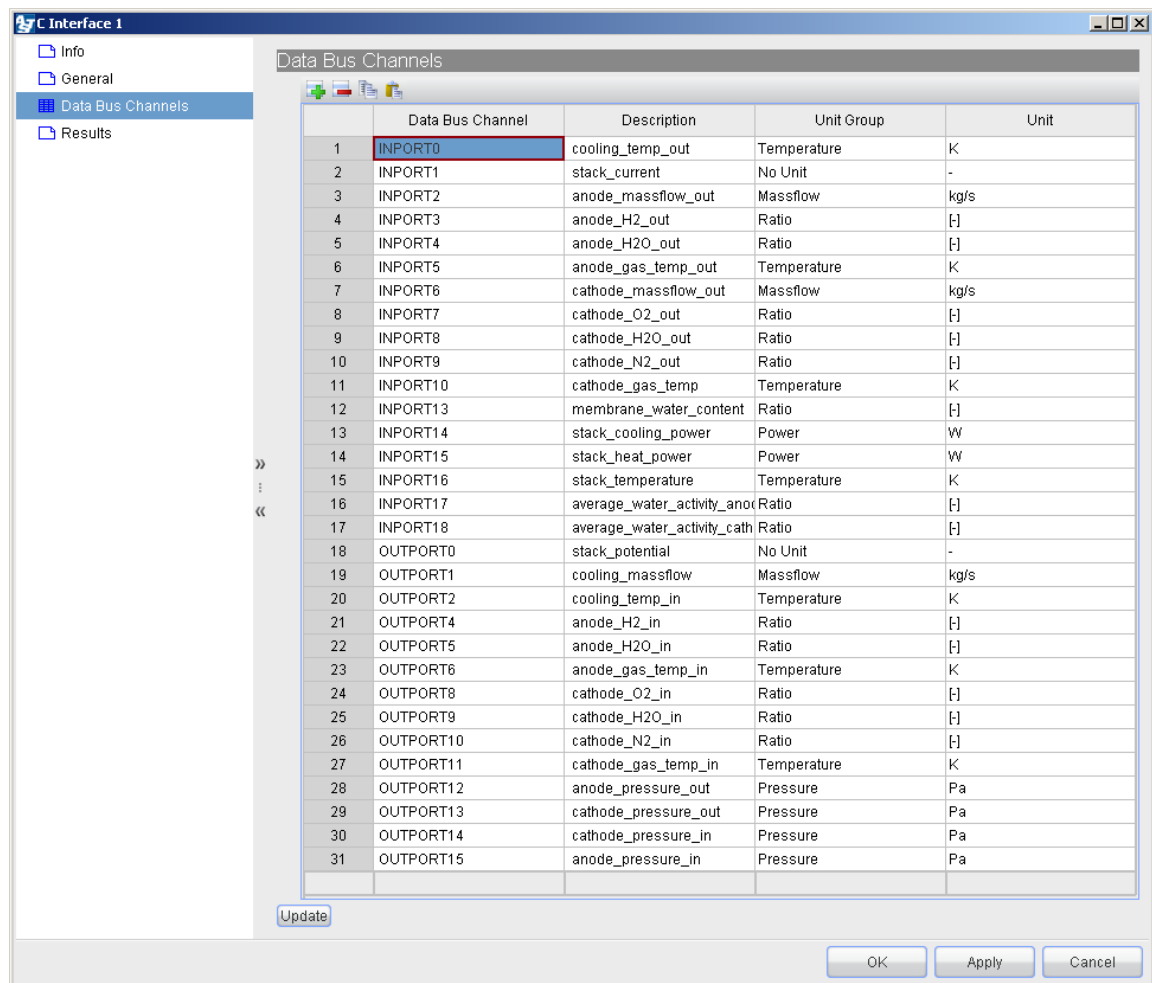


Figure 6.8: The C-Interface input and output ports

Furthermore, if one does not want to provide the data via the C-Interface, one just clicks on the value and the link is cut off. The elements then use the values provided in the user interface of the elements or they can be provided via Functions or other BOOST RT elements. The user can change the configuration and add or remove data links. The standard configuration of the Data Bus is set for a pressure driven model.

If the model has been changed into a mass flow-driven configuration, the Data Buses have to be changed too. Cut off the link where the pressure is provided for the inlet Ambients and set up a new connection to the multiplier of the mass flow element. The figure below shows the data link to the Anode inlet pressure via the C-Interface output.

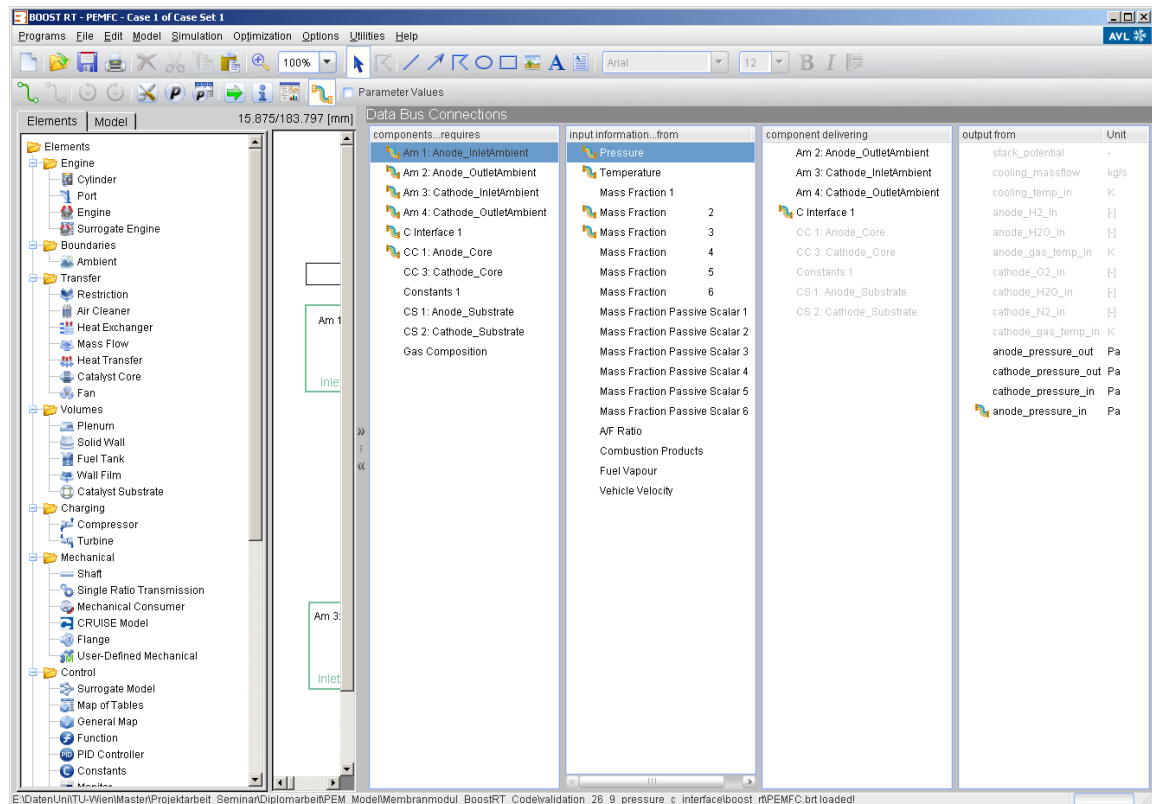


Figure 6.9: Data Bus Connections

As already mentioned, the C-Interface links the inputs and outputs to Matlab/Simulink via the model data buses of BOOST RT. If desired, the user can edit these connections. For instance, if deterioration of the fuel cell is taken into account, the model-specific parameter which is affected by deterioration can be added as data bus in the C-Interface and varied over time by an input of Matlab/Simulink.

Finally, when the entire configuration has been done, the model compilation is carried out. This step is necessary to transfer the model from the BOOST RT environment to Matlab/Simulink. At the end of the compilation, the model appears as a block in Simulink, where all the predefined inputs and outputs from the C-Interface show up. Then the BoP components can be linked to the model.

To establish the compilation go to “Simulation → CMC “. Choose the platform in

which the model should run. Therefore, switch to Matlab S-function 32bit or 64bit and change the number from 1 to 0 in the options Folder and Task. Afterwards press the start button. The compilation procedure executes all the steps and the process is finished when Matlab/Simulink opens and shows the model in the Simulink environment.

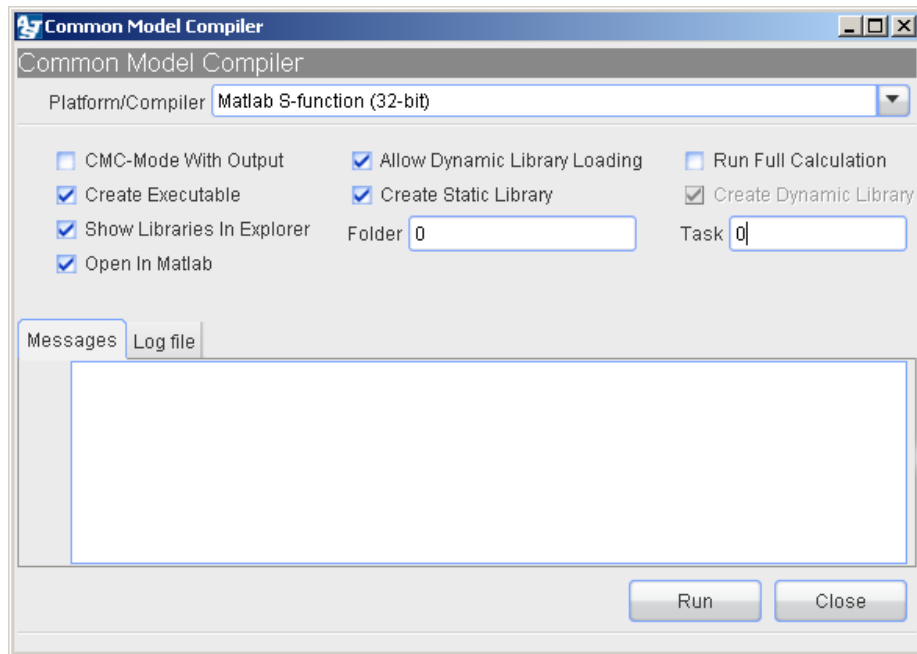


Figure 6.10: CMC element

After having run a simulation the user can look at the simulation results by starting the IMPRESS Chart and opening the folders where the simulation results are being stored. Then the results can be investigated and manipulated to create plots of different kinds, like a plot with the Current Density along the Channel. Basically for every element a folder exists where the user can investigate certain data. The PEM Core specific data is stored in a folder named "PEM Fuel Cell" which is found in the folder "Anode → Anode_Substrate". The figure below shows the opened PEM Fuel Cell folder and all fuel cell specific data that can be investigated.

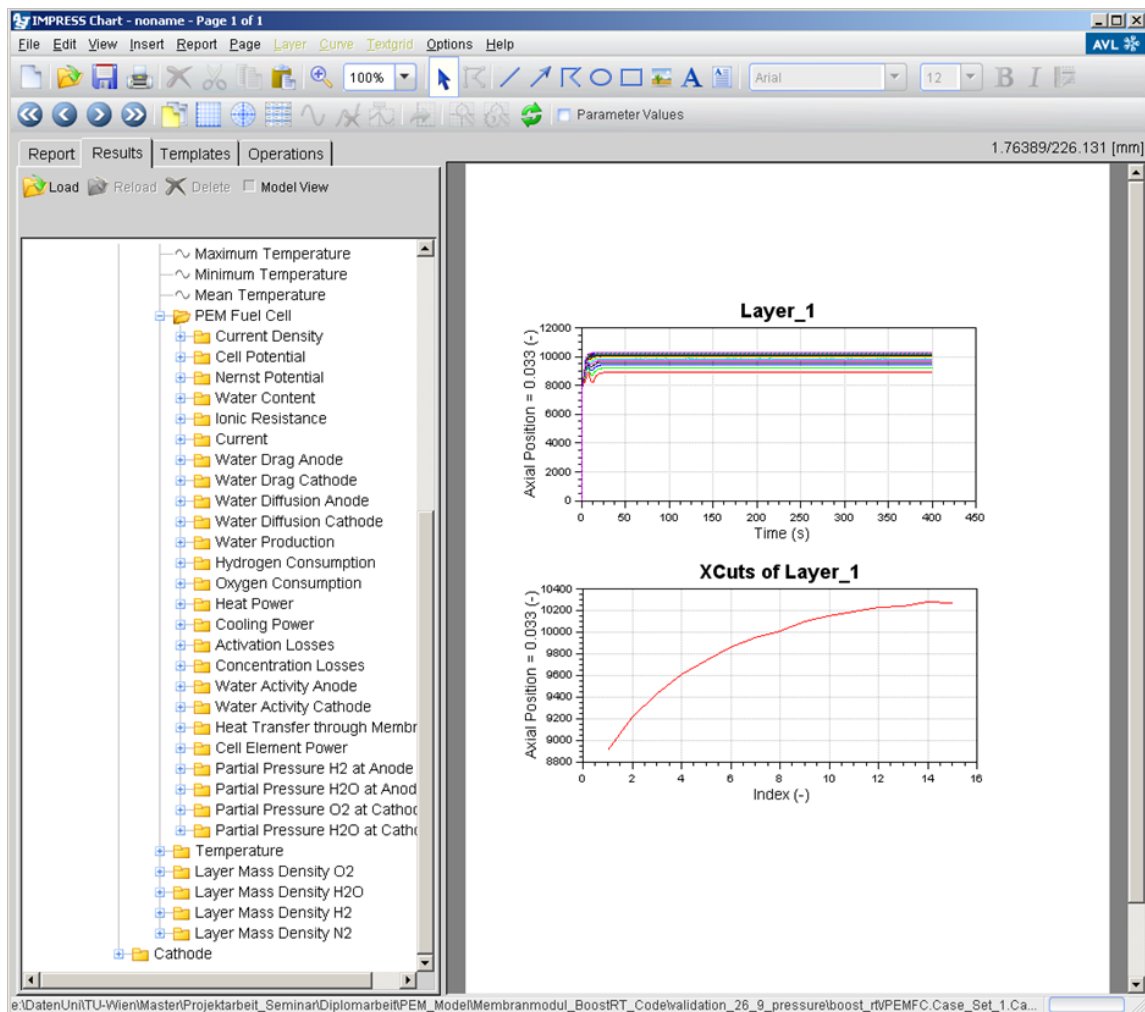


Figure 6.11: The IMPRESS Chart

6.2 Model Configuration and Fitting

This section comprises the model configuration and fitting of a single real PEM fuel cell. The PEM model is configured to a reference operation case which defines the basic boundary conditions. Then the effects of the variation of several different boundary conditions are investigated and it is documented how the model is able to cope with the variations. Finally the simulation results are compared to the measurements of the experiment and interpreted.

If values are separated by a "/" sign then the left value counts for the anode and the right value counts for the cathode side. If the gas humidification is cited as 0.6/0.9 that would mean a 60% humidification on anode and a 90% humidification on cathode side.

At the beginning the user has to decide whether a pressure or a mass flow-driven model fits the boundary conditions better. In this case the model was chosen as pressure driven. Normally the input data comes from Simulink but when it comes to the fitting of the model it is recommended to provide the input data via the BOOST RT environment. This option provides a faster access to the model parameters. The final configuration for the validation is shown in figure 6.12.

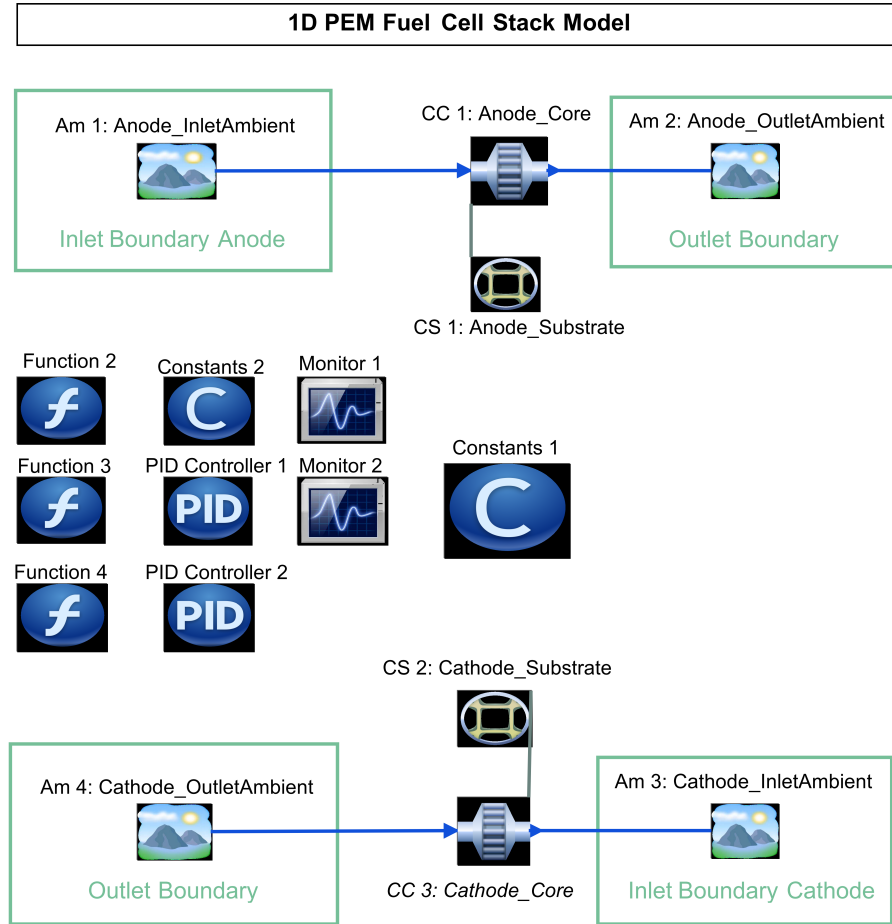


Figure 6.12: Model configuration

The additional key elements, which are not included in the basic configuration, are Functions, Constants and PID controllers. Via the Data Bus Connections option all the ports, of the additional elements, are linked together. In addition the data connections to the C-Interface have to be disabled. The Functions calculate variables and provide constant input data which are linked via the Data Bus Connections to different BOOST RT elements.

A Function element can be used instead of Simulink to provide input and output data. The outputs are calculated by using C-Code methods which are encoded in the GUI of the Function. So Function 2 calculates the lambdas of anode and cathode.

Function 3 and 4 calculate mass fractions for the Ambient Inlet elements and the water humidification levels of the input gas streams.

The value λ stands for the stoichiometry. It describes the amount of a supplied gas in relation to the actual consumption in the cell. λ is positive, has no unit and can be evaluated for the anode and the cathode side. If it is lower than one the chemical reactions will collapse.

The PID controllers execute pressure variations in view of the desired lambdas. PID 1 adjusts the pressure of the Anode Inlet Ambient and PID 2 does the same at the Cathode Inlet Ambient.

Finally, the Constants 2 block provides mass fractions of water for anode and cathode.

6.2.1 The PEM Fuel Cell and the Reference Case

The reference literature for the validation is the work of Fink [1]. Fink has set up a precise 3D model of a single PEM fuel cell which had been built in reality. Different operating scenarios have been measured and compared to the outcomes of the 3D model. This cell is modeled in BOOST RT and most of the previously discussed steps are executed through the calibration procedure. The 3D model is shown in figure 6.13.

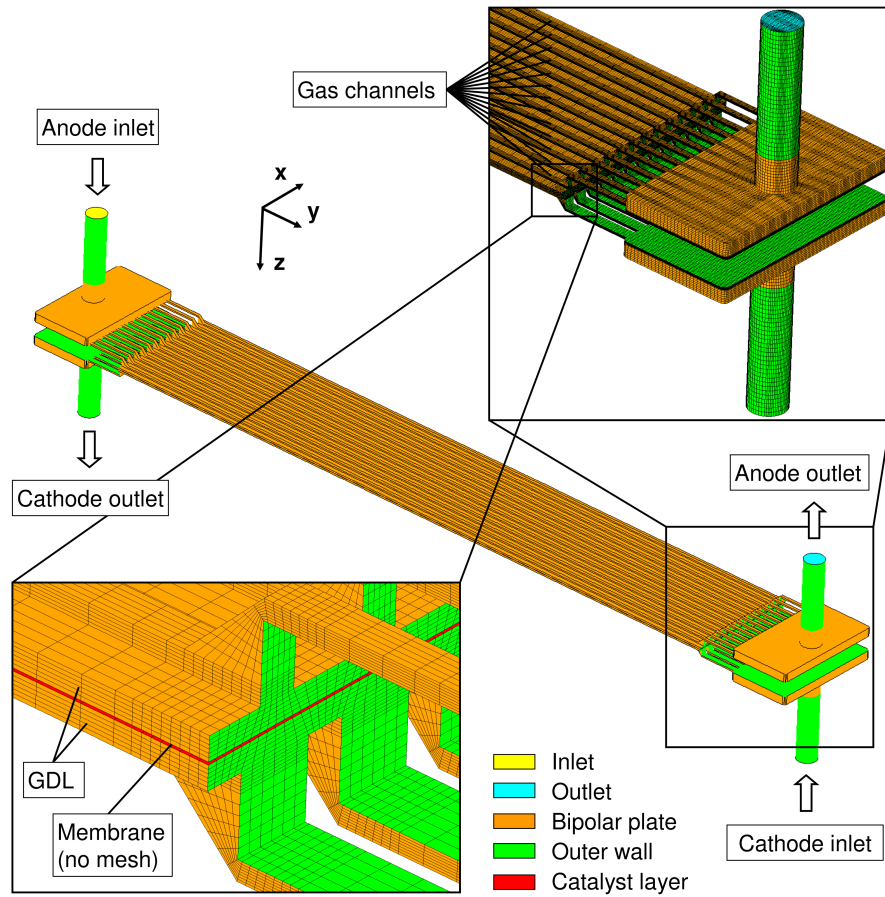


Figure 6.13: PEM fuel cell used for the validation [1]

The figure shows that the real system consists of one single cell. However, the figure does not show the huge cooling plates which ensure a precise temperature control of the cell itself. The cooling system was able to sustain a relatively constant temperature throughout the cell. Furthermore, the gases on the anode side flow in the positive y direction whereas the gases at the cathode side flow into the negative y direction. Keep that in mind when investigating the coming figures where a coordinate is depicted as the channel length. The exact physical data of the cell is listed below:

Physical data of the PEM fuel cell	
Number of Cells	1
Reactive Cell Area	25 cm^2
Length of Cell	120 mm
Width of Cell	20.8 mm
Numer of Gas Channels	13/13
Height and Width of an Anode Gas Channel	0.25 x 0.5 mm
Height and Width of a Cathode Gas Channel	0.25 x 1 mm
Height of the Cell (calculated)	$2 \times 0.3125 \text{ mm}$

The height of the cell is a value that has to be determined. As the Catalyst Core simulates gas streams streaming to drilled surfaces. Regarding the cell dealt with here, the starting point was the open area in front of the entry site of the gas channels. The open area was 25% on anode side and 50% on cathode side. The calculation below shows how the height of the cell was calculated.

$$Height_{Cell} = 2 \cdot \frac{\frac{13 \cdot 0.25 \cdot 0.5}{0.25}}{20.8} = 2 \cdot \frac{\frac{13 \cdot 0.25 \cdot 1}{0.5}}{20.8} = 2 \cdot 0.3125 \quad (6.4)$$

The experiment is carried out with different pressures, humidity levels and different lambdas. At the beginning the model is fitted to the reference case which has the following configuration. Furthermore, the parameters are varied to meet the new boundary conditions.

Boundary Conditions		
Anode Inlet	Stoichiometry Relative humidity Inlet gas temperature	$\lambda_{anode} = 1.5$ $\phi_{anode.in} = 0.9$ $T_{anode.gas.in} = 70^\circ\text{C}$
Anode Outlet	Outlet pressure	$P_{anode.out} = 101\,325\text{ Pa}$
Cathode Inlet	Stoichiometry Relative humidity Inlet gas temperature	$\lambda_{cathode} = 2.2$ $\phi_{cathode.in} = 0.9$ $T_{cathode.gas.in} = 70^\circ\text{C}$
Cathode Outlet	Outlet pressure	$P_{cathode.out} = 101\,325\text{ Pa}$
Cooling Fluid	Fluid temperature Mass flow	$T_{cooling.in} = 69^\circ\text{C}$ $\dot{m}_{cooling.in} = 0.244\text{ kg}\cdot\text{s}^{-1}$
Cell	Solid temperature	$T_{cell} = 70^\circ\text{C}$

Considering these boundary conditions the experiment was carried out. The polarization curve measured during the experiment is shown in figure 6.14. This is the main polarization curve and all the free parameters are varied until the simulation results of the model fit the polarization curve of the experiment. This is done in the next section where all the free parameters are chosen.

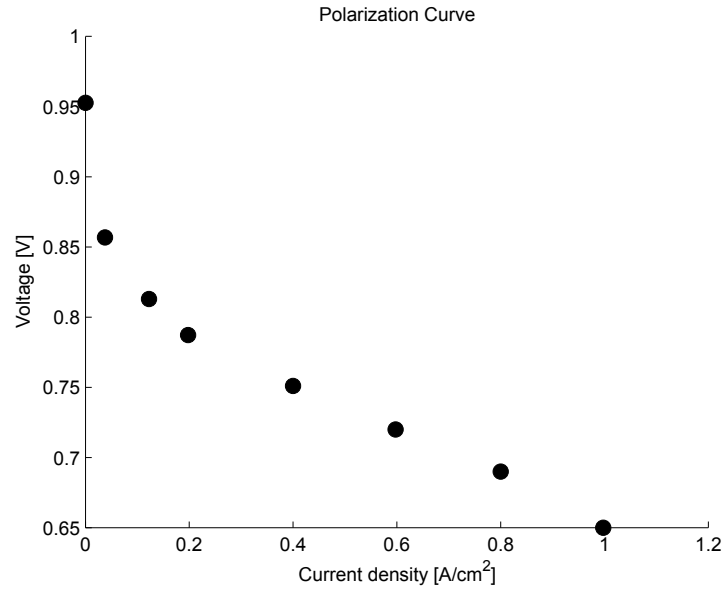


Figure 6.14: Reference case experiment measurements

6.2.2 BOOST RT GUI Parameters for the Reference Case

In the last part the polarization curve of the reference case has been shown. As an automatic fitting algorithm was not available, the fitting of the polarization curve of the model had to be done manually. How the single parameters influence the evolution of the polarization curve has been explained in great detail in the work of Barbir [4]. Basically, the activation losses are responsible for the initial fall of the curve, ohmic and ionic losses are responsible for the fall in the mid section and the parameters of the limiting current influence the sharp drop at the end of the curve.

The following figures show the final parametrization of all the free parameters. The exact meaning of all the constants and how they are calculated has already been described. The Catalyst Core and Catalyst Substrate elements were configured in the following way:

CC 1: Anode_Core

General

Length	0.12	m
Volume	7.8e-007	m ³
Catalyst Type Specification	Input of hydraulic diameter, OFA and GSA	
CPSI	400	1 / in ²
Wall Thickness	0.0001778	m
Hydraulic Diameter	0.000333	m
Open Frontal Area	0.25	[-]
Geometrical Surface Area	3000	1 / m
Flow Coefficient	1	[-]
Friction Specification	Coefficient	
Mass Flow	1e-005	kg / s
Inlet Temperature	343	K
Inlet Pressure	110000	Pa
Target Pressure Drop	1000	Pa
Turbulent Friction Coefficient	0.019	[-]
Laminar Friction Coefficient	64	[-]
Friction Multiplier	0.65	[-]
<input type="checkbox"/> Transient Momentum Balance		
Inertia Multiplier	1	[-]

OK Apply Cancel

Figure 6.15: Reference case anode Catalyst Core configuration

CS 1: Anode_Substrate

General

Washcoat Thickness	1e-015	m
<input checked="" type="checkbox"/> Axial Discretization		
Number of Grid Points	15	
Grid Shape Factor	1	[-]
Initial Temperature	343	K
<input checked="" type="checkbox"/> Variable Temperature		
Solid Material	Graphite	

OK Apply Cancel

Figure 6.16: Reference case anode Catalyst Substrate configuration

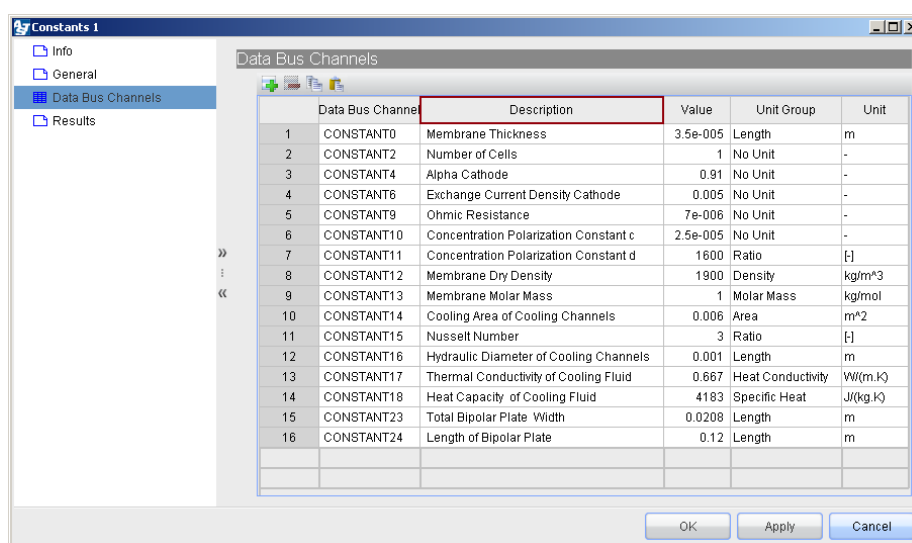
Parameter	Value	Unit
Length	0.12	m
Volume	7.8e-007	m ³
Catalyst Type Specification	Input of hydraulic diameter, OFA and GSA	
CPSI	400	1 / in ²
Wall Thickness	0.0001778	m
Hydraulic Diameter	0.0004	m
Open Frontal Area	0.5	[-]
Geometrical Surface Area	5000	1 / m
Flow Coefficient	1	[-]
Friction Specification	Coefficient	
Mass Flow	0.0002	kg / s
Inlet Temperature	343	K
Inlet Pressure	110000	Pa
Target Pressure Drop	1000	Pa
Turbulent Friction Coefficient	0.019	[-]
Laminar Friction Coefficient	64	[-]
Friction Multiplier	0.95	[-]
Transient Momentum Balance	<input type="checkbox"/>	
Inertia Multiplier	1	[-]

Figure 6.17: Reference case cathode Catalyst Core configuration

Parameter	Value	Unit
Washcoat Thickness	1e-015	m
Axial Discretization	<input checked="" type="checkbox"/>	
Number of Grid Points	15	
Grid Shape Factor	1	[-]
Initial Temperature	343	K
Variable Temperature	<input checked="" type="checkbox"/>	
Solid Material	Graphite	

Figure 6.18: Reference case cathode Catalyst Substrate configuration

As far as the Friction Multipliers are concerned, they were determined with the knowledge of the pressure drop at 1000 Pa/2700 Pa on anode and cathode at an operating voltage of 0.69 V. This pressure drop resulted from switching the Friction Multipliers to 0.65/0.95. The last parameters are those concerned with the PEM Core and are configured via the Constants 1 element.



Data Bus Channel	Description	Value	Unit Group	Unit
1	CONSTANT0 Membrane Thickness	3.5e-005	Length	m
2	CONSTANT2 Number of Cells	1	No Unit	-
3	CONSTANT4 Alpha Cathode	0.91	No Unit	-
4	CONSTANT6 Exchange Current Density Cathode	0.005	No Unit	-
5	CONSTANT9 Ohmic Resistance	7e-006	No Unit	-
6	CONSTANT10 Concentration Polarization Constant c	2.5e-005	No Unit	-
7	CONSTANT11 Concentration Polarization Constant d	1600	Ratio	[-]
8	CONSTANT12 Membrane Dry Density	1900	Density	kg/m^3
9	CONSTANT13 Membrane Molar Mass	1	Molar Mass	kg/mol
10	CONSTANT14 Cooling Area of Cooling Channels	0.006	Area	m^2
11	CONSTANT15 Nusselt Number	3	Ratio	[-]
12	CONSTANT16 Hydraulic Diameter of Cooling Channels	0.001	Length	m
13	CONSTANT17 Thermal Conductivity of Cooling Fluid	0.667	Heat Conductivity	W/(m.K)
14	CONSTANT18 Heat Capacity of Cooling Fluid	4183	Specific Heat	J/(kg.K)
15	CONSTANT23 Total Bipolar Plate Width	0.0208	Length	m
16	CONSTANT24 Length of Bipolar Plate	0.12	Length	m

Figure 6.19: Reference case Constants 1 configuration

This was the configuration of the model. Now all the different operating scenarios can be tested which will be done in the next section.

6.3 Model Validation

The Model Validation shows the comparison of the simulation with the outcomes of the experiment. Three different cases are carried out. In the first case the pressure is varied. The second case comprises the variation of the stoichiometric flow ratio and the third case shows the effects of different relative humidity levels.

6.3.1 Simulation of the Reference Case

The outcome of the simulation of the reference case is shown in figure 6.20.

The simulation time for every voltage level was 100 seconds. The data analysis yielded, that at lower voltages the boundary conditions were perfectly met. On the other side, at 0.751 V the λ of the cathode, which was 2.2, could not be met anymore. The next step then was to investigate the current density along the channel. At the operating point of 0.690 V detailed data was available from the 3D simulation. So the operating points at 0.751 V and 0.690 V were plotted, which is exhibited in the figure 6.21. Starting at 80 mm the simulation results point to higher current densities than in the experiment which means higher activity in this area of the cell. The plot shows clearly that this tendency increases with higher voltages and after a certain operating level the model needs a higher λ to find a steady solution.

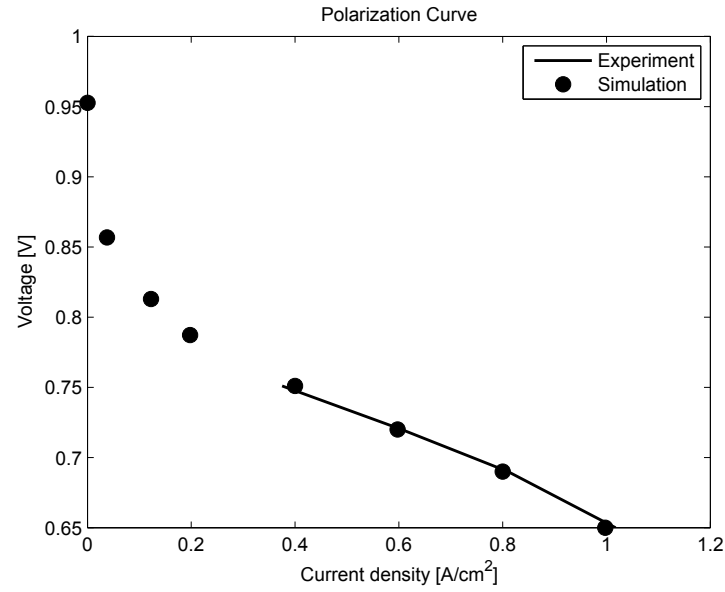


Figure 6.20: Simulation of the reference case

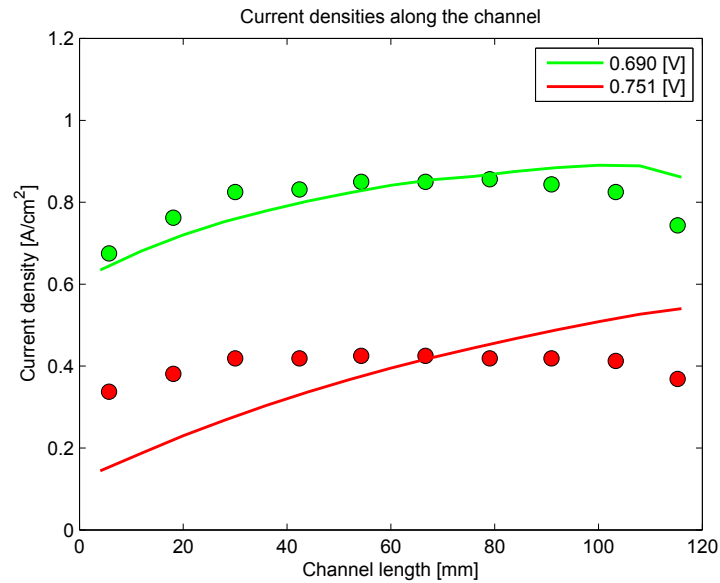
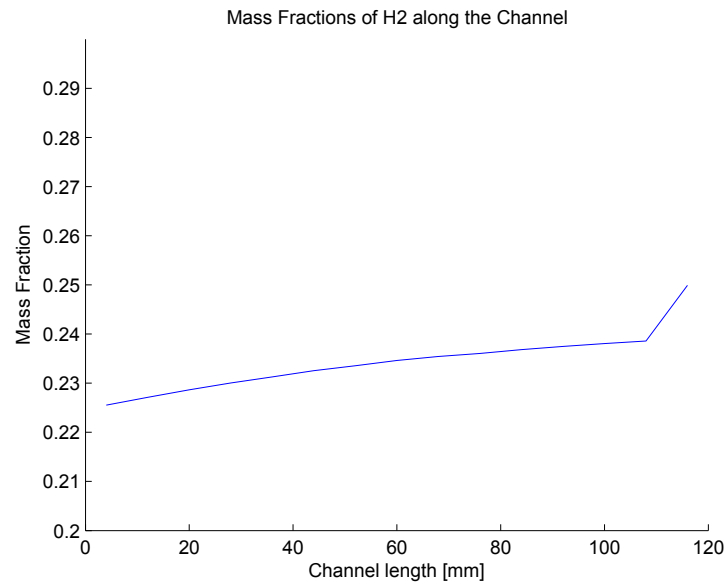
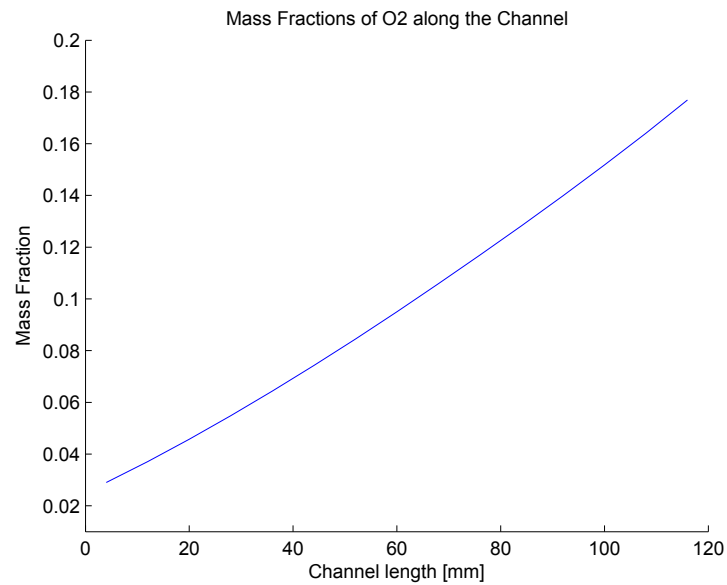


Figure 6.21: Current densities along the channel

The next step was to create a plot of the mass fractions of H_2 on the anode and O_2 on the cathode side at 0.690 V. The data is displayed in figure 6.22 and 6.23. A comparison of the plots to the outcomes of the 3D model has shown that on the cathode the mass fractions tendency is correct but the simulation points to a much deeper drop of the mass fraction than in the 3D model. The anode side does not at all fit to the outcomes of the 3D model.

Figure 6.22: Mass fractions of H_2 Figure 6.23: Mass fractions of O_2

As the main problem the mass stream of the Catalyst Core was identified. At the operating point of 0.690 V the mass stream on anode side goes down by 60% and the cathode mass stream increases by 5%. In the model, though, the Catalyst Core assumes a constant mass stream. In the simulation of catalytic reactions in the after-treatment of exhaust gas systems this assumption can be made. However, in

the simulation of PEM fuel cells, gas streams are significantly affected by sink and source terms and that leads to partial pressures which cannot be compared to those of constant mass streams. The mass stream on cathode side could be assumed constant but on anode side definitely not. So in the simulation there is a higher hydrogen partial pressure at the end of the anode gas channel than in the experiment, which leads to higher current densities. Sink and source terms are implemented in the calculation core and appear in the Catalyst Substrate and therefore they have an effect on the Catalyst Core elements but the Catalyst Core fills the missing mass to get the constant mass stream. The results are wrong mass fractions and partial pressures which have significant influence on the performance of the cell and the distribution of the current densities along the channel.

As far as the model is concerned, the reason why it was not possible to simulate higher voltages is the mass fraction of O_2 on cathode side. In the cathode gas channel outlet region, which is at 0 mm, the mass fraction is already at 0.02. If the boundary conditions of the cell are now changed to a level where the gas velocity or mass stream in the gas channel goes down, the mass fraction further decreases. The mass stream goes down because the driving pressure difference goes down. That is because the model tries to find a steady solution with lambda 2.2. This process of lowering the inlet pressures continues until the all the current densities have finally reached zero. To sum up, at a certain voltage level the model is not able to find a steady solution with a constant lambda anymore e.g. lambda of 2.2 at 0.751 V in the given case.

The figures 6.24, 6.25, 6.26 show certain model parameters developing over time. In every plot the voltage has been increased every 100 seconds as in the reference case depicted, from 0.650 V to 0.787 V.

The steady states are found at least after 50 seconds. But starting at the step to 0.751 V the model was not able to find a steady state anymore. The mass fraction of O_2 or the partial pressure in the last element of the cathode, where the gasses leave the gas channel, goes down rapidly. The mass stream on cathode side is then too high due to the drop of the current density in the cell and the inlet pressure is lowered, which leads to a lower mass stream. This continues until the average current density has fallen to zero which means that the model is not able to find a steady state at 0.751 V with a lambda of 2.2. The only way now to reach a steady operating point is to change the boundary conditions. In the case of 0.751 V a steady solution was found at a lambda of 2.37.

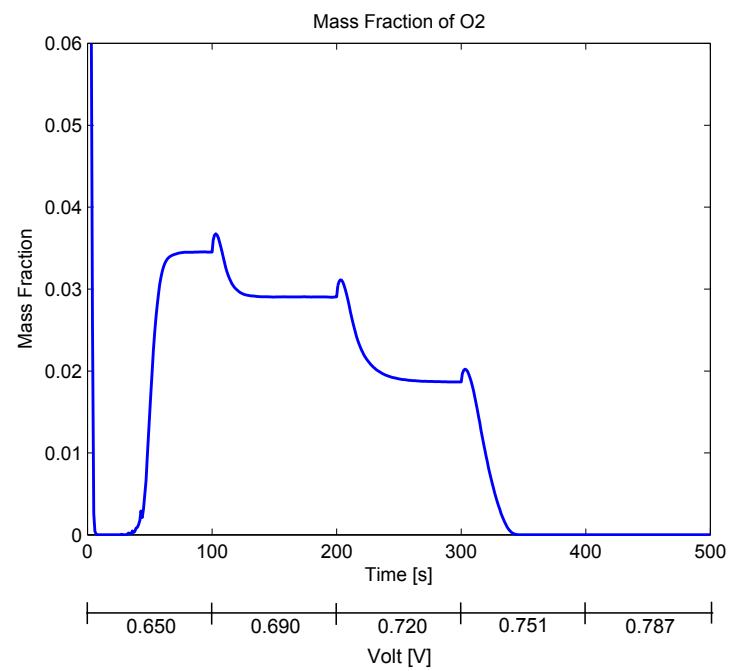


Figure 6.24: Mass fraction of O_2 in the last cathode gas channel element

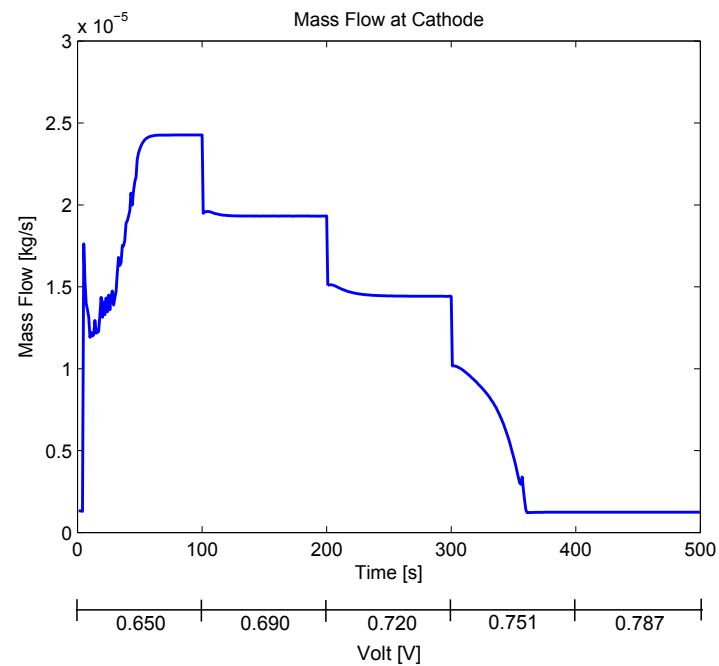


Figure 6.25: Mass flow in the cathode gas channel

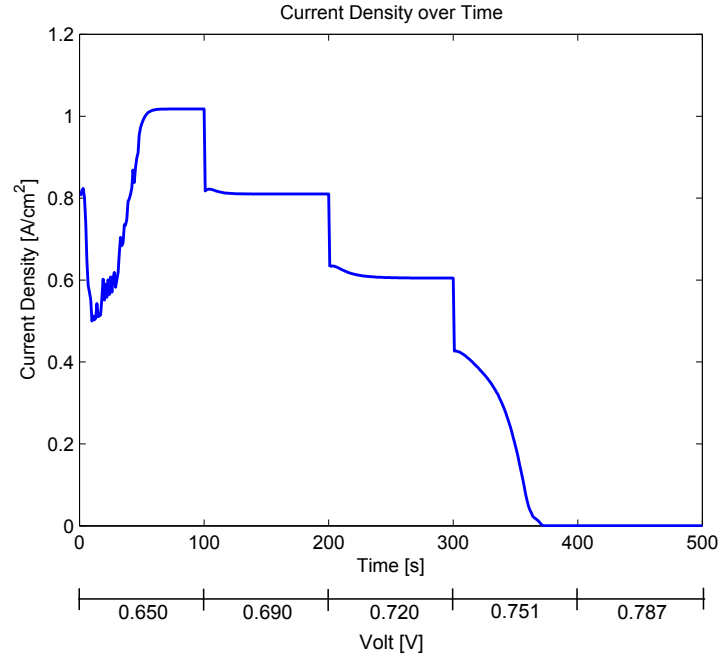


Figure 6.26: Cell average current density plotted over time

The next chapter shows how the model copes with different boundary conditions. Again the focus is on the mass stream and on how the various changes of the boundary conditions lead to an increase or a decrease of the mass stream.

6.3.2 Pressure Variation

This section shows how the model is capable of simulating different pressure scenarios. Therefore, the outlet pressures were changed at both gas channels. Basically, a PEM fuel cell reaches higher power levels with higher pressures due to higher Nernst potentials and higher exchange current densities. One of the disadvantages of higher pressures is the leakage of species out of the cell or through the membrane. However, the mapping of these effects is not included in the model. Regarding the variation of the boundary conditions, only those indicated here are changed whereas the rest stays constant.

Boundary Conditions		
Anode outlet	Outlet pressure	$P_{anode.out} = 121325 \text{ [Pa]}$
Cathode outlet	Outlet pressure	$P_{cathode.out} = 121325 \text{ [Pa]}$

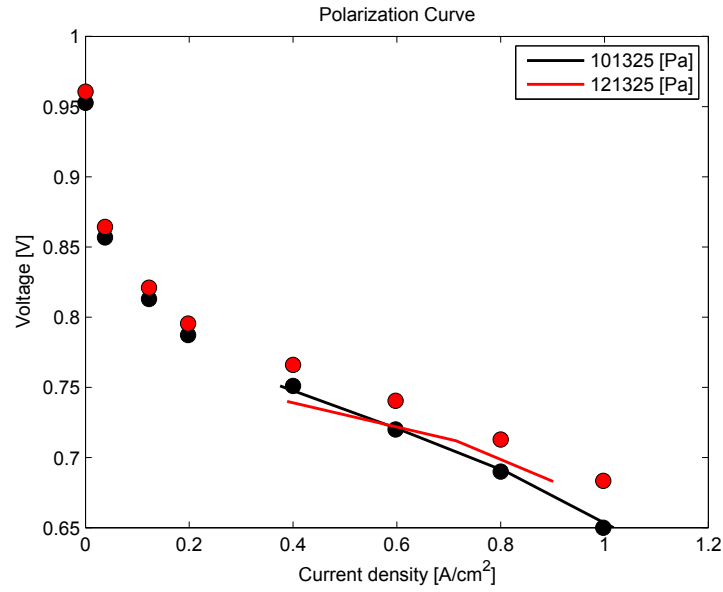


Figure 6.27: Simulation at 1.2 bar

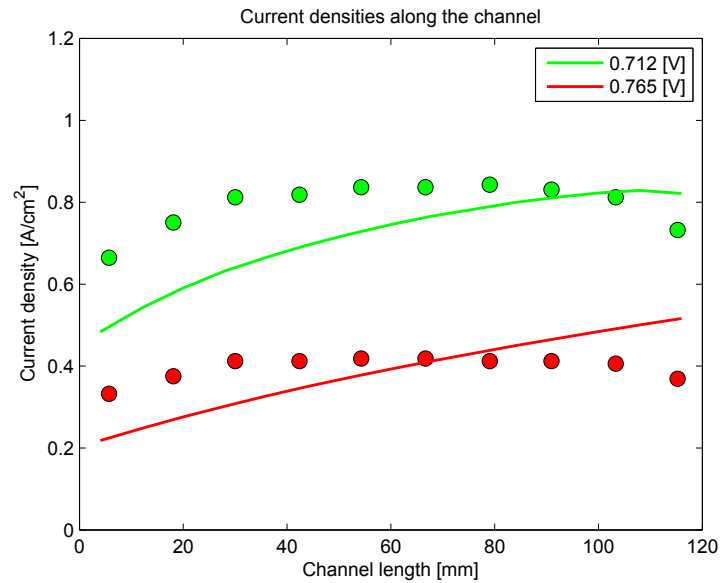


Figure 6.28: Current densities along the channel

There is significant divergence between the current densities of the simulation and the experiment. Compared to the reference case, the mass flow has now fallen at higher voltages and the model was not able to find a steady state at 0.740 V. At least a lambda of 2.5 was necessary to find a steady point. Nevertheless, the experiment results have shown higher mass streams due to the fact that at higher pressures the current densities increase under a constant voltage.

The next scenario is the change of the humidification on both sides.

6.3.3 Different Humidification

This scenario investigates how the polarization curve is influenced by a change of the inlet gas humidification at both electrodes. Basically a higher humidification leads to higher current densities due to higher water contents of the membrane which results in lower ionic resistances. The major disadvantage, is the risk of cell flooding, which leads to a collapse of the reactions. Now the humidification is lowered from 0.9/0.9 to 0.6/0.6, which leads to lower current densities at constant voltages.

Boundary Conditions		
Anode	Relative humidity	$\phi_{anode.in} = 0.6$
Cathode	Relative humidity	$\phi_{cathode.in} = 0.6$

The simulation has produced the following results:

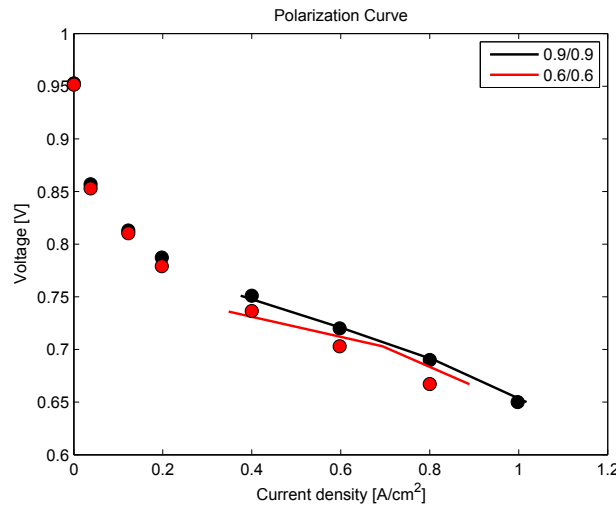


Figure 6.29: Simulation at 0.6/0.6

The simulation shows a unsatisfactory fit with the experiment. The drop of the current densities should be deeper than in the simulation. The reason is that the lowering of the humidification level does not sufficiently affect the water content or ionic resistance. That is a consequence of the constant mass stream.

The plot of the current densities along the channel, though show a better fit except the fact that the current densities are too high. There the lower humidification leads to more concave curves than in the reference case which is in line with the experiment's outcome. At higher voltages, though, the curve rise sharpens. When

simulating a voltage of 0.736 V at least a lambda of 2.34 was necessary to establish a steady state.

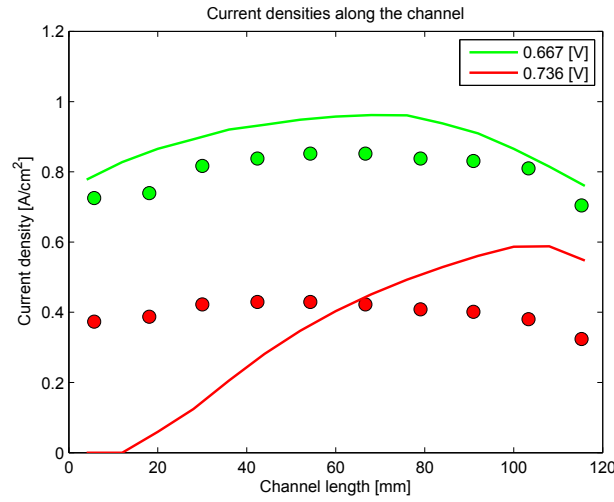


Figure 6.30: Current Densities along the channel

To sum up, a drop in the humidification level of the inlet gasses should lead to lower current densities. As the model simulates a constant mass stream, which is not the case in the experiment, more water is transported than in the experiment. Consequently, the ionic resistance is lower and the cell performs differently in the simulation.

In the last scenario the stoichiometry is changed and simulated.

6.3.4 Different Stoichiometry

In this section the stoichiometry of the cell is changed from 2.2 to 4 on cathode side. A higher lambda results in higher mass streams and gas velocities and the model should better fit to the experiment due to the assumption of a constant mass stream.

Boundary Conditions		
Cathode Inlet	Stoichiometry	$\lambda_{cathode} = 4$

The simulation has shown the following result:

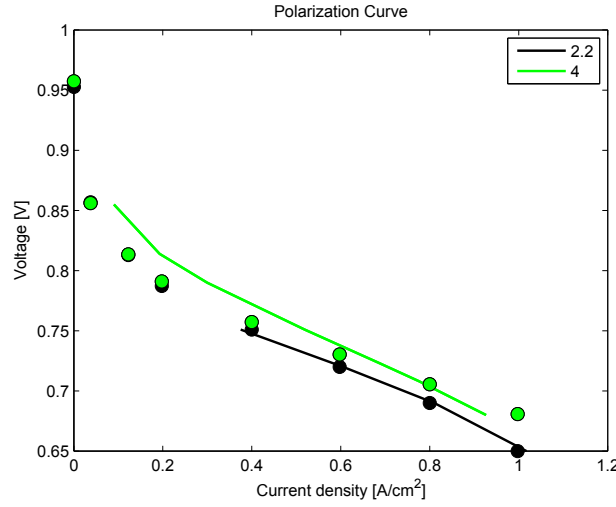


Figure 6.31: Simulation with lambda 4

The simulation shows a significant better fit compared to the other scenarios. All cases which have been investigated, have pointed to lower mass streams and gas velocities and higher mass changes along the channel. Now as the lambda has been increased the mass stream can be considered rather as constant parameter than in previous cases. This is in shape with the simulation's outcomes. The model was able to simulate lower current densities than in the reference case.

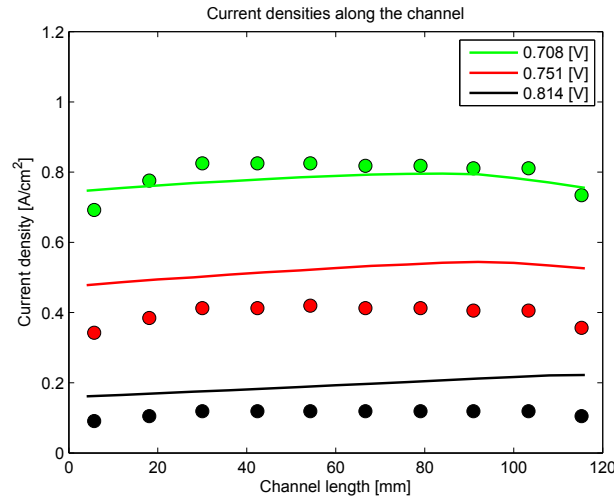


Figure 6.32: Current densities along the channel

The current densities are in line with the statements. The experiment points to flatter current density curves along the channel, which corresponds to the simulation's outcomes. Nonetheless, the fall of the current densities at the channel inlet and outlet is not sufficiently mapped and at higher cell voltages the average current densities

are too high.

This was the last operating scenario of the PEM fuel cell. The next section sums up all the general and model-related findings of this thesis.

6.4 Result Interpretation and Compendium

The main outcomes of the thesis can be split into findings regarding the general modeling of PEM fuel cells and the model specific findings.

It can be claimed that PEM fuel cells cannot be accurately modeled when constant mass streams in the gas channels of anode and cathode are suggested. The gas stream is considerably influenced by sink and source terms, which have an effect on the mass balance of the gas channels. Hydrogen is transported from anode to cathode and water is transported via diffusion and the drag effect. It depends on the boundary conditions of the cell if the mass flow rises or sinks through the gas channel of either anode or cathode. As the rise or fall of the mass can be considerable, the modeling of PEM fuel cells with constant mass streams lead to significant divergences with the outcomes of the experiment.

Regarding the model-specific outcomes, the comparison of the simulation with the experiment can be summed up as follows: All the different scenarios showed that with the increase of the mass stream, which is in line with the rise of the gas velocity, the simulation better fits to the experiment than with a fall of the mass stream. Especially higher lambdas showed better fits. In all scenarios, though, the fits of the current densities along the channel were satisfactory at higher current densities. At lower current densities the simulation led to better conditions at the cathode gas channel entry area of the cell. This is mainly due to the constant mass stream where the model simulates higher activity at the anode gas channel outlet area of the fuel cell.

Despite these divergences, the model provides a good basis for further developments. It demonstrates how a 1D model of a PEM fuel cell can be structured.

Finally the last chapter gives an overview of possible further model developments.

Chapter 7

Possible further Model Development

As the previous section has shown, the model provides a good structure for simulating PEM fuel cells but the mass stream cannot be assumed as constant. The strengths of the model are the interoperability with Matlab/Simulink, a comfortable configuration and real time simulations. Furthermore the C-Code calculation core allows comfortable adaptations of the algorithm.

7.1 Catalyst Core Adaptations

The next step of the model development should focus on how the assumption of a constant mass stream can be canceled. A good solution would be a new element. This element could either replace the Catalyst Core only or is an entirely new coded element which could replace Core and Substrate. A clear advantage of this option is that the new code could be supplemented with existing code fragments. Besides, another advantage is that this new gas channel element could be optimized for PEM fuel cell gas channels. In particular, the existing Catalyst Core element assumes that the whole gas channel wall is reactive, as this is the case within an exhaust catalyst core. In a fuel cell only one side of the channel is next to the porous medium. Furthermore, the reactions start at the beginning of the porous substrate element. The gases diffuse through the GDL and then reach the catalytic site where the reactions occur. This behavior of the gases in the channels has to be considered if the user wants to simulate sophisticated dynamic behavior of the fuel cell.

7.2 Advanced Membrane Model

A second possible future development is the improvement of the membrane model which calculates the ionic resistance related to the water content of the membrane. Currently the calculation of the ionic resistance is based on the work of Zawodzinski [29]. Here the water content is calculated from the knowledge of the water activity on anode and cathode side but it does not consider any dynamics regarding the ionic

resistance. According to Wang, see [21] and [31], the electrodynamics of the PEM fuel cell are mainly influenced by the membrane. If higher precision is demanded regarding the dynamic behavior of the cell, e.g. for a more accurate control of the BoP components, the membrane model should be further improved. As the membrane calculation is coded in C-Code this could be comfortably done via code adaptations.

Bibliography

- [1] Clemens Fink. Modelling and simulation of multiphase transport phenomena in porous media with application to pem fuel cells. 2009.
- [2] Ballard Power Systems. <http://www.ballard.com/>.
- [3] Christoph Hartnig, Ingo Manke, Robert Kuhn, Sebastian Kleinau, Jürgen Goebbels, and John Banhart. High-resolution in-plane investigation of the water evolution and transport in pem fuel cells. *Journal of Power Sources*, 188(2):468–474, 2009.
- [4] Frano Barbir. *PEM fuel cells: theory and practice*. Academic Press, 2012.
- [5] LO Vasquez. *Fuel cell research trends*. Nova Publishers, 2007.
- [6] <http://de.wikipedia.org/wiki/naion>. *Wikipedia.org*, 2013.
- [7] Viral Mehta and Joyce Smith Cooper. Review and analysis of pem fuel cell design and manufacturing. *Journal of Power Sources*, 114(1):32–53, 2003.
- [8] Colleen Spiegel. *PEM fuel cell modeling and simulation using MATLAB*. Academic Press, 2011.
- [9] Richard Hanke-Rauschenbach. *Strukturierte Modellierung und nichtlineare Analyse von PEM-Brennstoffzellen*. PhD thesis, Otto-von-Guericke-Universität Magdeburg, Universitätsbibliothek, 2007.
- [10] PR Pathapati, X Xue, and J Tang. A new dynamic model for predicting transient phenomena in a pem fuel cell system. *Renewable energy*, 30(1):1–22, 2005.
- [11] <http://www.mathworks.de/>. Mathworks, 2013.
- [12] <https://www.avl.com/home>. 2013.
- [13] <http://www.mec.tuwien.ac.at>. 2013.
- [14] Jens Niemeyer. *Modellprädiktive Regelung eines PEM-Brennstoffzellensystems*. Univ.-Verlag Karlsruhe, 2008.
- [15] U Stimming. Grundlagen der brennstoffzellen-technologie, brennstoffzellen-typen und ihre anwendung. *VDI BERICHTE*, 1174:237–237, 1995.

- [16] Chunshan Song. Fuel processing for low-temperature and high-temperature fuel cells: Challenges, and opportunities for sustainable development in the 21st century. *Catalysis Today*, 77(1):17–49, 2002.
- [17] Kristina Haraldsson and Keith Wipke. Evaluating pem fuel cell system models. *Journal of Power Sources*, 126(1):88–97, 2004.
- [18] Frieder Herb. *Alterungsmechanismen in Lithium-Ionen-Batterien und PEM-Brennstoffzellen und deren Einfluss auf die Eigenschaften von daraus bestehenden Hybrid-Systemen*. PhD thesis, Dissertation, Universität Ulm, 2010.
- [19] <http://de.wikipedia.org/wiki/polytetrafluorethylen>. *Wikipedia.org*, 2013.
- [20] Xianguo Li and Imran Sabir. Review of bipolar plates in pem fuel cells: Flow-field designs. *International Journal of Hydrogen Energy*, 30(4):359–371, 2005.
- [21] Yun Wang and Chao-Yang Wang. Dynamics of polymer electrolyte fuel cells undergoing load changes. *Electrochimica Acta*, 51(19):3924–3933, 2006.
- [22] Yun Wang, Ken S Chen, Jeffrey Mishler, Sung Chan Cho, and Xavier Cordobes Adroher. A review of polymer electrolyte membrane fuel cells: Technology, applications, and needs on fundamental research. *Applied Energy*, 88(4):981–1007, 2011.
- [23] Clemens Fink and Nicolas Fouquet. Three-dimensional simulation of polymer electrolyte membrane fuel cells with experimental validation. *Electrochimica Acta*, 56(28):10820–10831, 2011.
- [24] Paul W Majsztrik, M Barclay Satterfield, Andrew B Bocarsly, and Jay B Benziger. Water sorption, desorption and transport in nafion membranes. *Journal of Membrane Science*, 301(1):93–106, 2007.
- [25] AVL List GmbH. <https://www.avl.com/web/ast/solutions>.
- [26] AVL List GmbH. https://www.avl.com/c/document_library.
- [27] Phong Thanh Nguyen, Torsten Berning, and Ned Djilali. Computational model of a pem fuel cell with serpentine gas flow channels. *Journal of Power Sources*, 130(1):149–157, 2004.
- [28] Thomas E Springer, TA Zawodzinski, and Shimshon Gottesfeld. Polymer electrolyte fuel cell model. *Journal of the Electrochemical Society*, 138(8):2334–2342, 1991.
- [29] Thomas A Zawodzinski, Thomas E Springer, John Davey, Roger Jestel, Cruz Lopez, Judith Valerio, and Shimshon Gottesfeld. A comparative study of water uptake by and transport through ionomeric fuel cell membranes. *Journal of the Electrochemical Society*, 140(7):1981–1985, 1993.

-
- [30] Junbom Kim, Seong-Min Lee, Supramaniam Srinivasan, and Charles E Chamberlin. Modeling of proton exchange membrane fuel cell performance with an empirical equation. *Journal of the Electrochemical Society*, 142(8):2670–2674, 1995.
- [31] Yun Wang and Chao-Yang Wang. Transient analysis of polymer electrolyte fuel cells. *Electrochimica Acta*, 50(6):1307–1315, 2005.